Final Technical Report (FTR)

a. Federal Agency	Department of Energy
b. Award Number	DE-EE0007165
c. Project Title	Agent-Based Coordination Scheme for PV Integration (ABC4PV)
d. Principal Investigator	Soummya Kar Professor soummyak@andrew.cmu.edu (412) 268-8962
e. Business Contact	Teri McCort teriz@andrew.cmu.edu (412) 268-3730
f. Submission Date	Friday, March 6th, 2020
g. DUNS Number	05-218-4116
h. Recipient Organization	Carnegie Mellon University
i. Project Period	**Start**: 01/01/2016 **End**: 12/31/2019
j. Submitting Official Signature	

Acknowledgement:
This material is based upon work supported by the U.S. Department of Energy's Office of Energy Efficiency and Renewable Energy (EERE) under the Sustainable and Holistic IntegratioN of Energy Storage and Solar PV (SHINES) Award Number DE-EE0007165.

Disclaimer:
This report was prepared as an account of work sponsored by an agency of the United States Government. Neither the United States Government nor any agency thereof, nor any of their employees, makes any warranty, express or implied, or assumes any legal liability or responsibility for the accuracy, completeness, or usefulness of any information, apparatus, product, or process disclosed, or represents that its use would not infringe privately owned rights. Reference herein to any specific commercial product, process, or service by trade name, trademark, manufacturer, or otherwise does not necessarily constitute or imply its endorsement, recommendation, or favoring by the United States Government or any agency thereof. The views and opinions of authors expressed herein do not necessarily state or reflect those of the United States Government or any agency thereof.

Executive Summary

Renewables and especially photovoltaics (PV) have benefitted significantly from a host of incentives and policies targeted toward enhanced integration and adoption of specific energy technologies. However, with the push to move forward into a subsidy-free market framework, behind-the-meter residential PV applications have generally struggled to retain their value (unlike utility scale and commercial projects) [1]. This project focused on developing control-theoretic solutions aimed at improving the integration and interaction of behind-the-meter residential PV with other distribution system assets (controllable and non-controllable) to enhance the *integrated value* of residential PV.

To this end, a suite of decentralized control methodologies have been developed to enable effective coordination and control of behind-the-meter residential load customers' PV, battery storage systems (BSS), controllable loads and other similar assets within a distribution feeder. This interaction aims at procuring energy savings and, thus, energy bill savings. The main source of savings is drawn from reducing the effect of demand charge pricing and is realized at the feeder level, assuming community level interaction and management among the aforementioned assets. Optimal control of the assets is implemented with a distributed optimization methodology, leveraging consensus-based algorithms. The results gathered from the optimal control simulations demonstrates that the savings can be duly achieved and the algorithm decision times (to dynamically control asset set points, for example) are fast.

As for the overall efficiency of PV+BSS systems, to procure energy savings from curtailment of the demand charge pricing effects, the optimal control is set up so as to minimize the variance of the load for all customers, throughout a feeder and throughout time in a rolling horizon scheduling with model predictive control. The control takes into account inter-temporal electrochemical storage (battery) degradation costs: specifically, we have developed a long-term lifetime model for the BSS that weighs in the effect of the degradation factor in the dispatch formulations, thus, a considerable operating cost that affects energy decision making. The levelized cost of energy (LCOE – redefined for the purpose of quantifying asset integration effectiveness through the customers' energy cost) is shown to be below the threshold set for the combined PV+BSS topology of $ 0.14/kWh for multiple cases of PV penetration all the way up to 50%, provided that a policy of shared ownership of and savings is in place. Further, the LCOE calculated for the case before the deployment PV+BSS systems is also achievable, i.e. the deployment of PV+BSS, if planned and scheduled optimally. will have no effect on customers' energy costs.

From the control methodology viewpoint, the developed consensus-based algorithms are shown to converge for a wide range of problem cases (spanning normal operating scenarios and contingencies), guaranteeing dispatch solutions under forecasting errors, communication break-downs and cyber-security attacks. The proposed control solutions are scalable and real-time implementable, with dispatch computations and device set-point updates converging in less than 2s in most practical instances of the above events.

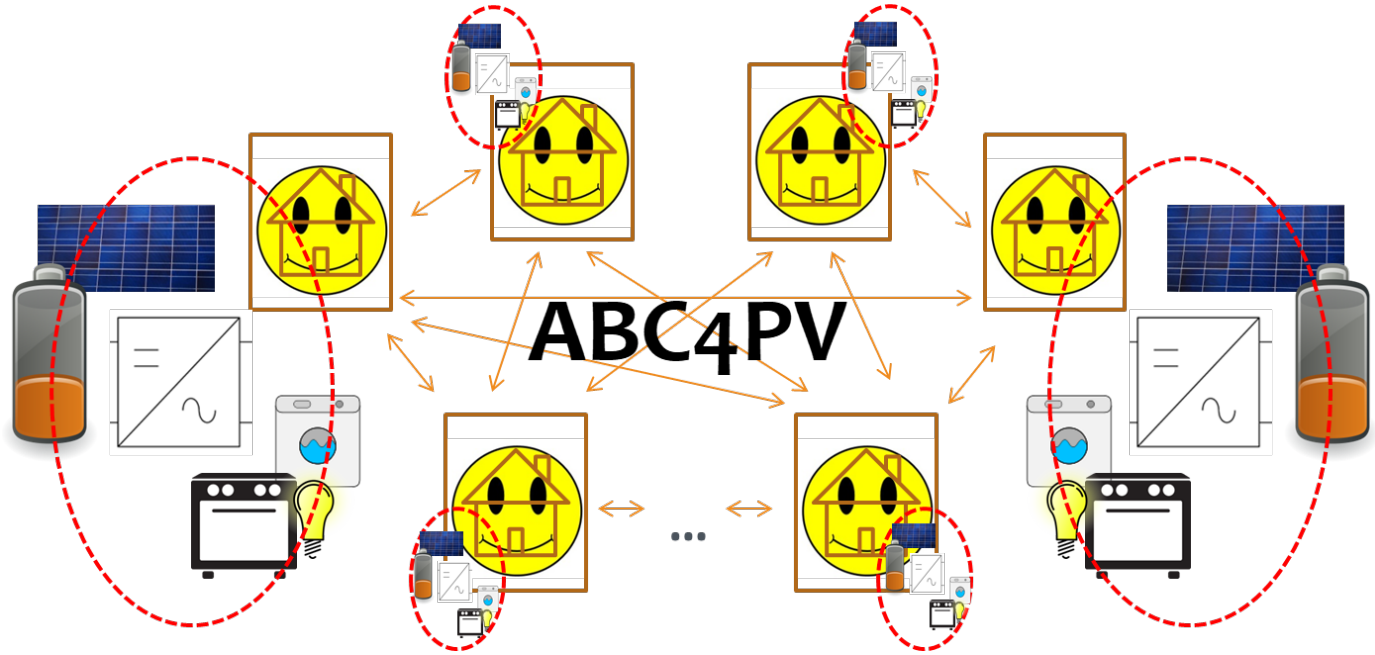

Fig. 1. The agent-based coordination of PV, BSS and interruptible loads in the distributed optimization ABC4PV framework.

Background

In order to properly assess the work undertaken in this project, two main R&D directions are identified, namely energy management objectives and optimal control tools.

Energy Management of Photovoltaics & Batteries for Residential Customers' Savings

The first issue of concern involves objectifying and understanding the socio-economic implications of coordinated optimal control of assets such as photovoltaics (PV), battery storage systems (BSS) and controllable loads installed in various end-customer points (mostly households) throughout a distribution network. This framework implies access to system monitoring and some direct control over end-customers' assets. Based on the rationale that large fleets of behind-the-meter (BTM) customers can better benefit from holistic PV+BSS management, this specification is made clearer by our focus on cooperatively owned and operated feeders. Thus, the literature review presented in the following is motivated by advances in the field of the optimal control and operation of fully vertically controlled distribution feeders and microgrids.

A second issue of concern is the ability to realistically quantify trade-offs between battery operating cost (due to its degradation) and optimal scheduling/dispatch. The working hypothesis sought to balance arbitrage opportunities (taking advantage of low cost energy generation deferred to time slots of more expensive energy) while also providing back-up power benefits to end-users in cases of emergency.

In light of the above points, we review the following relevant literature. Compared to [2] the cost objective devised in this work takes into account various PV energy pricing systems and is built on a battery degradation model for a more realistic consideration of its effect on the cost. Additionally, we consider demand response capabilities of loads. A relevant approach in this context is also considered in [3], with a simplified battery operation cost. The allocation and operation of Distributed Generation (DG) units, which enforce capital cost considerations in the objective function are discussed in [4]; this is in contrast with the hypothesis assumed in this project, that PV-storage deployment in households is predetermined. In the context of this project, the coordinated (optimal) control of the units deployed, rather than PV-storage placement infrastructure design, is envisioned to incentivize wider penetration of the proposed "plug-and-play" philosophy to end-customers' households. Some analysis on the net-metering policy on PV energy is conducted in [5] and a detailed battery degradation model is used in [6]. However, the battery degradation model used is in the interest of the operating constraints of the storage system and not as a cost-contributing factor in the decision-making. Instead of PV-energy billing, green certificates are considered in [7], while the degradation cost of the storage system is not accounted for; nevertheless, a linear factor on the performance of the PV installation and operating the storage system in that regime, could be considered as a simplified approach to the issue. A net metering policy is assumed in [8] and weights are assigned on each of the cost terms of the objective function (optimizing both on operating costs and line losses). A detailed cost operating model for the battery storage system, which is shown to be convex, is assumed in [9]. Although any approach to quantify the cost of Electric Vehicle (EV) batteries may be, practically, intractable, we commented on [10], as it attempts to coordinate the operation of DG, EV storage and interruptible loads, so as to minimize infeed costs, while satisfying trip plans of the Electric

Vehicles. Although [11] is a risk aware scheduling technique to cover for the stochastic nature of wind generation through other sources, neither the charging efficiency nor the degradation cost of the battery storage are accounted for. Similarly, the approaches presented in [12, 13] are risk-aware, the former by incorporating penalties in the objective function and the latter by enforcing the relevant constraints. Neither of these studies weighs in on the operating cost of the storage system. A problem quite similar to the one addressed in this project has been discussed in [14] but for thermal generation and restricted to net-metering billing policy. A linear approximation of the battery degradation cost as obtained in [15] has been used for this study. In [16] redundant energy and emission costs from EVs, thermal generation, DG and loads capable of demand response have been coordinated, in the absence though of any credible degradation cost model for the EV storage. The aforementioned publications on optimal resource scheduling suffer mainly in the context of:

i. Properly addressing the subsidy-free PV energy assumption, and

ii. Quantifying the operating cost of the battery storage system due to its degradation.

The work conducted in this project accounts for both of these issues in an attempt to develop optimal scheduling of the battery utilization and load management at the level of system wide control of multiple units.

We elaborate further on certain critical aspects of the cost objective considered in this project. The revenue that may be procured by exploiting the role of battery storage systems as energy buffers of the PV output in a subsidy-free policy framework, has to be based on a load pricing policy that is not flat. If energy rates are not flat (demand charge, time of use – TOU – tariffs, peak pricing, etc.), exploiting the potential of batteries as energy buffers can benefit users by shifting their consumption from expensive times of a certain period to cheaper ones. In wider scopes, such shifting has been proposed through methods like peak shaving, valley filling and others. As it is implied by these latter points, batteries dispersed over a microgrid among end-users may serve both emergency loads when seldom interruptions occur and procure savings through energy shifting. In the context of this work, we considered the Demand Charge Pricing as the most challenging policy of the aforementioned type. Unlike TOU tariffs, Demand Charge Pricing (DCP) is applied retroactively. Under DCP, after a clearance period has come to an end (usually a calendar month in length), for the hour of that period that the peak loading for a given feeder has occurred, all active loads of that feeder are subject to an extra cost. This extra cost is orders of magnitude greater than the typical energy cost. For example, in the case of an average, actual cooperative feeder (the cooperative acts as an aggregator for all participating parties, mostly households, connected to the feeder), which will also be discussed later in the analysis, DCP is $40/kWh, while the energy cost is around $0.07/kWh. It is evident that if some proper handling of the loads is used, the total energy cost for the end users will be notably reduced. To achieve that, loads should be shifted away from peak times to valley times, BSS could store energy at valley times and feed load around peak times, etc. However, focusing on the peak loads does not ensure energy saving for the community microgrid per se, due to the fact that DCP is applied retroactively and over a long clearance period. To properly handle the effects of DCP, firstly, we consider any available DG assets as “negative loads” (as for microgrid battery storage, according to the flow of energy), and, following in this sense, the proposed control solution seeks to minimize the variance of the augmented set of “loads”

of the community microgrid. Load variance minimization (LVM), which is equivalent to minimizing energy losses [17], has emerged mostly from the valley filling strategy for EV charging and will be briefly reviewed here. Traditionally, LVM has been posed as a quadratic programming problem of minimizing the variation of flexible loads (behind a point of common coupling or of a whole feeder) about their daily average or a target profile [17-22]. LVM is usually decoupled from the economic dispatch of DG, BSS and DR resources. Shaving peak loads and shifting them to valley times through TOU tariffs [23, 24] or other pricing methods [25-27] and rule/heuristic mechanisms [28, 29], are means to approximate LVM in a non-explicit manner. In the context of this work, LVM is extended to minimize the joint variation of all loads and DG (load-generation variation minimization – LGVM) installed on a cooperative feeder operating as a community microgrid. The microgrid battery storage is employed as a buffer for DG that is shifted to peak times, so that the overall "apparent" load of the feeder (not to be confused with apparent power) is minimized about its daily average. This way, the effect of DCP to the total energy cost for the microgrid becomes negligible.

Distributed Optimization Framework

The algorithmic approach used and developed in this project, "Consensus + Innovations" (C+I), requires a separate concise review on its realizations in distributed optimal control problems.

Consensus-based approaches that exploit information from neighboring actors in optimal power management problems has recently received notable attention [30, 31] due to their decentralized nature, scalability and flexibility. In its earlier versions [32-35], researchers proposed decentralized solutions for the economic dispatch (ED) problem (i.e. neglecting line constraints) by enforcing a consensus on the marginal cost of generation through an iterative process. However, line congestion would render the marginal costs unequal and, thus, the aforementioned algorithm is unable to handle the Optimal Power Flow (OPF) problem, since it contains line constraints. To handle this challenge, [36] suggested an innovation based approach. The core of this method is based on iterative updates which solve the first order optimality conditions associated with the OPF problem. The original optimization problem may be solved through a coupled system of equations. Optimality conditions involve solely local information, hence the variable updates in C+I for the considered problem could be performed in a fully decentralized fashion. To this end, the optimality conditions are integrated as innovation updates in the variable updates. In this approach, each bus just exchanges information with its physical neighbors, i.e., other buses that are physically connected through transmission lines. It should be noted that the set of parties/actors, performing optimization in the C+I framework, need only a connected communication network (i.e. there is at least one path between any pair of nodes/parties/actors). We note that the realizations of the distributed C+I based control obtained in this project does not take into account:

i. the bus voltages limits and the effect of reactive power to their regulation,

ii. the effect of line resistances (common also in most linearized OPF approaches [37]), due to the fact that they are usually of negligible magnitude compared to the line reactance's.

The mathematical formulation devised in the ABC4PV ensures that the proposed control can both cater to the dispatching of reactive power in terms of voltage regulation, as also account for the resistive nature of distribution network lines.

Project Objectives

The high-level objective of this project is to develop the technology and operating framework to deploy integrated photovoltaics, storage, and load control (including thermostats) in a way that realizes greater value than either the individual components deployed on their own or single integrated combination of PV, storage, and load control operating independently of other such deployments.

Specific scientific and technological objectives and outcomes of this project include:

1. Design and development of a holistic control methodology for effective integration of distributed generation, storage and load control and its implementation to the specific instance of PV, battery storage and programmable thermostats and plug load controllers. The proposed methodology is distributed, agent-based and achieved optimal control and coordination of resources in distribution feeder systems. Also, it is :
   - Scalable, by employing an agent-based control paradigm in which local decisions at the system entities are determined through simplistic local computations and peer-to-peer information exchange;
   - Generic, i.e., provides optimal control synthesis for a wide range of distribution feeder systems based on operational characteristics of the various system entities;
   - Risk-aware, i.e., the optimal control settings take into account uncertainties associated with solar and load variability and their forecasts;
   - Robust, i.e., able to cope with intermittent malfunctioning of local agent computational processes and occasional failures in inter-agent communication.
2. Mathematical analysis of the distributed control methodology including optimum design and cost-of-operation assessment as a function of the operational characteristics of the feeder network, the installed controllable components and the quality of load and solar forecasting employed in the decision-making process.
3. Implementation and testing of the measures to ensure the cyber-security of the agents and the operating framework.
4. A software implementation of the control methodology in a high-level programming language (MATLAB and/or C++) to extensively simulate control performance (i.e., overall cost required to achieve reliable energy dispatch) over a wide range of system parameters and operating conditions: specifically, we considered varying generation-demand-storage cost curves, varying storage specifications, how performance varies with varying uncertainty-attributes modeling load and solar forecasting, and, in particular, identify system and device configurations that achieve the LCOE target operation cost in a socio-technologically reliable fashion.
5. An open-source assessment of an actual feeder in the Open Modeling Framework (OMF), NRECA's GridLAB-D based simulation platform, for showing the existing concerns for system support by PV+BSS systems. The OMF implementation emulated a scenario very close to actual operation. To achieve the above, the OMF environment has been extended as follows (which might be of independent interest, as well):

- Simulation of an actual feeder with real year-long data. This is done in the extended OMF for a feeder at a co-op which has agreed to participate as a partner in the project by making a feeder available for testing. The simulation modeled the performance of the feeder in response to different weather scenarios, electricity prices, and electrical demand on the feeder and the broader utility. For each scenario, the model showed the technical and financial performance of residential customers and their power quality.

6. A testbed/prototype development of the distributed resource coordination and control algorithms by means of deploying networked "ABC4PV units" on CMU campus for full scale field demonstration of the agent-based ABC4PV solution.
   - Development of the agent hardware, interfacing the agent to the battery, storage, and load controller(s) and to communicate with each other in a distributed fashion;
   - Installation and physical setup of PV arrays, storage and flexible demand on the test feeder and implementation of the agent algorithms on the dedicated hardware;
   - A detailed techno-economic assessment of both the entire system as well as the energy storage subsystem attributed to the implementation of the proposed control methodology.

   The test-bed of CMU campus units was further emulated in the MATLAB platform to assess the energy exchanges scheduling and examine concerns for communication breakdowns and cyber-attacks. The results corroborated our expectations and theoretical guarantees with respect to the major project objectives.

7. Development in control and energy system decision-making methodologies achieved in this project have been published in high-impact peer-reviewed national and international conferences and journals. We proposed and chaired special sessions in major energy and control conferences to promote and disseminate our research results in this field.
8. The PIs were invited to present the work at special sessions of conferences and give seminars at academic and industrial organizations including energy utilities and co-ops. These events made the broader energy community aware of the technology and the demonstration and promoted its further development and adoption.

Project Results and Discussion

The results of our efforts are organized and presented by Task.

Task 1: Design and Development of Distributed Resource Coordination and Control Methodology

• High-level description of research and outcomes: *The objective function describing the day-ahead cost of covering the end-customer loads has been determined. The capabilities of the unit (PV energy, storage and interruptible loads) have been incorporated in the function. The technical, operating and policy limits have been expressed through constraints. Contracted PV energy is proposed as a subsidy-free alternative to net-metering. A novel C+I formulation that solves the scheduling problem for distribution systems with voltage concerns has been developed. Proof of convergence has been produced for the iterative, distributed, optimal scheduling algorithm. Extensive tests have been conducted for convergence assessment.*

Each residential customer is equipped with BTM PV+BSS systems the operations of which come at certain costs that need to be minimized for maximum savings. At the same time, those customers have load costs from the operation of their devices. The following costs are identified for the system assets:

- ***PV power* has zero operational cost**. The stochastic availability of solar irradiation implies that any de-loading of a PV system incurs missed opportunity cost and reduced revenue (because of degrading monetary value for PV energy that is deferred to later time). Hence, Maximum Power Point operation is realized [38]. That said, the component degradation is inevitable and cannot affect its operational cost which is zero for the PV Modules and the PV Inverter.
- ***Battery storage* operational cost is two-fold** and is broken down as follows:
  - The **cost of the battery recharging current** depends on the electricity rate and/or any available excess of Distributed Generation (DG) that may be used. Charging efficiency might be a concern if not otherwise accounted for.
  - The **battery degradation cost** represents a major part of the operational cost. The decision on the depth of discharge (DoD) and, hence, on the charging schedules of the storage system affects both the future availability of battery capacity and also its lifetime. Unlike previous studies, the battery degradation cost in this project is related to the usage profile, which may not be considered given and constant for the whole duration of the storage lifetime. *Battery degradation is formulated below.*
- The ***cost of load*** is calculated **at two levels:**
  - The **load to be served** at any given time depends on the electricity rate, and the available DG and storage that can be deployed to this end.
  - The **load to be interrupted** has a cost that follows a specific rate according to a pre-agreed contract with the end-user(s) or a similar demand response plan.

Based on the above discussion, the objective function of the scheduling problem is:

$$\text{minimize} \quad f = \left[\sum_{i\in\{loads\}} P_{i,L,t} + \sum_{i\in\{batteries\}} \frac{P_{i,RCh,t}}{n_i} - \sum_{i\in\{PV\}} P_{i,NM,t} - \sum_{i\in\{batteries\}} P_{i,DCh,t} \right]_{t\in[1,24]}^{T} \cdot \left[IF_t\right]_{t\in[1,24]} +$$

$$+ \sum_{t\in[1,24]} \sum_{i\in\{batteries\}} Dgd_{i,RCh,t} + \left[\sum_{i\in\{loads\}} P_{i,IL,t} \right]_{t\in[1,24]}^{T} \cdot \left[ILC_t\right]_{t\in[1,24]} -$$

$$- \left[\sum_{i\in\{PV\}} P_{i,Cntr,t} \right]_{t\in[1,24]}^{T} \cdot \left[Cntr_{PV,t}\right]_{t\in[1,24]} \qquad \textbf{\textit{(I)}}$$

Where:

Ch:	Set of batteries recharging,
n_B:	Battery recharging efficiency (in per unit values or %),
DG,av:	Excess of DG available to recharge storage (in p.u. or kW),
Dch:	Set of discharging batteries,
Dgd:	Degradation cost (in $),
IF:	Energy In-feed cost (in $),
L-{IL}:	Set of load demand excluding interruptible load,
DG/B,av:	Excess of DG or storage available to serve load demand (in p.u. or kW),
L∈{IL}:	Set of interrupted load demand,
IL:	Interruptible load cost (in $).
$P_{i,L,t}$ & $P_{i,IL,t}$:	Part of i-th load consumed & interrupted, respectively, at hour *t* (in p.u. or kW),
$P_{i,RCh,t}$ & $P_{i,DCh,t}$:	Part of i-th battery recharged & discharged, respectively, at hour *t* (in p.u. or kW),
n_B:	Battery recharging efficiency (in p.u. or %),
$P_{i,NM,t}$ & $P_{i,Cntr,t}$:	Part of i-th PV on net-metering & contract tariffs, respectively, at hour *t* (in p.u. or kW),
IF:	Cost of in-fed energy (in $),
Dgd:	Degradation cost (in $),
ILC:	Interruptible load cost (in $),
$Cntr_{PV}$:	contracted price for photovoltaic energy (in $).

In the above, a day-ahead horizon formulation has been assumed. Moreover, the PV systems constitute the sole type of DG units considered in the setup. The IF and IL rates are given as vectors that are not flat. Besides the non-flatness of the IF and IL rates,

additional costs can be assumed to be added as penalties or incentives to shift loads, generation and storage. The framework of model predictive control [39], as this is referred to in the SOPO, further affirms this last assumption. From the formulation of the objective function (I) it follows that when an excess of storage and distributed generation occurs, there is a reimbursement equal to the infeed cost of energy. This has been derived by the assumption that net-metering policies [40] are in place. However, to strengthen the subsidy-free profile framework of the SUNSHOT initiative, we constrain the total amount of stored energy discharged in every unit to the total amount of load of the unit; i.e. no revenue is considered for stored energy fed to the grid. Secondly, the photovoltaic installation may or may not feed its energy to the grid, but at a contracted price with a local aggregator, utility owner, etc.

With regards to the constraints of the optimization problem the following are noted:

$$\underline{P^f_{PV,i,t}} \le P_{PV,i,NM,t} + P_{PV,i,Cntr,t} \le \overline{P^f_{PV,i,t}} \qquad \textbf{\textit{(II)}}$$

$$\underline{v_{batt,i}} \le v_{batt,i,t}\left(P_{batteries,i,RCh,t}, P_{batteries,i,DCh,t}, v_{batt,i,t-1}\right) \le \overline{v_{batt,i}} \qquad \textbf{\textit{(III)}}$$

$$0 \le P_{batteries,i,DCh,t} \le \overline{P_{batteries,i,DCh}} \qquad \textbf{\textit{(IV)}}$$

$$0 \le P_{batteries,i,RCh,t} \le \overline{P_{batteries,i,RCh}} \qquad \textbf{\textit{(V)}}$$

$$\underline{P^f_{i,L,t}} \le P_{i,L,t} - P_{i,IL,t} \le \overline{P^f_{i,L,t}} \qquad \textbf{\textit{(VI)}}$$

$$\sum_{t\in[1,24]} P_{i,IL,t} \le \overline{P_{i,IL}} \quad \text{or} \quad \sum_{t\in[1,24]} P_{i,IL,t} = 0 \qquad \textbf{\textit{(VII)}}$$

$$\underline{|v_i|} \le |v_i| \le \overline{|v_i|} \quad \text{and} \quad \underline{|S_{ij}|} \le |S_{ij}| \le \overline{|S_{ij}|} \qquad \textbf{\textit{(VIII)}}$$

$$p_{ij} - q_{ij} = \left(g_{ij} - b_{ij}\right)\cdot(\theta_i - \theta_j) \quad \text{and} \quad p_{ij}\cdot g_{ij} - |v_i|\cdot g_{ij}^2 + |v_j|\cdot g_{ij}^2 = q_{ij}\cdot b_{ij} + |v_i|\cdot b_{ij}^2 - |v_j|\cdot b_{ij}^2 \qquad \textbf{\textit{(IX)}}$$

$$P_i = \sum_j p_{ij}, \quad Q_i = \sum_j q_{ij} \qquad \textbf{\textit{(X)}}$$

Constraint (II) expresses the physical limits of the availability of photovoltaic power from the module installed. Due to the time-ahead horizon nature of the optimization problem, however, the maximum and minimum may not be defined, but estimated or forecasted (*f* superscript). Constraint (III) is the function describing the effect of a discharge or recharge action on the battery storage system to its voltage across the terminals, depending also on the voltage of the previous time slot. In a little more detail:

$$v_{batt} = E_0 - i\cdot\left(K\frac{Q_{\max}}{Q_{\max} - \sum_{k=1}^{T}|i_k|\cdot t_k} + R_0\right)$$

where,

v_{batt} : battery open circuit operating voltage (in p.u. or V)
E_0 : internal voltage (constant/characteristic of the battery, in p.u. or V)
i : charge/discharge current (signed, positive for discharge, in p.u. or V)
K, R_0 : resistant type constants (characteristics of the battery, in p.u. or Ω)
t : total time of applying i to the batter, for multiple different i's
Q_{max}: maximum capacity of the battery.

The next two constraints outline the maximum discharging and recharging currents of the battery storage system. We note, as presented previously, that these also depend on the operating limits of the power electronics device to which the storage system is connected to. Constraint (VI) describes the limitation on the amount of load that can be interrupted as a portion of the load at the time. The minimum allowed load is, essentially, the critical load that cannot be shed at the time, while the maximum allowed load includes any additional load that can be used at the time. The latter makes sense if the interruptible load is shifted at different times of the day and which, in turn, relates to constraint (VII). If there is no load-shifting considered, there will be a constraint of a total amount of load that can be shed throughout the scheduling horizon. If the practice for the interruptible load is to shift it at different times of the day, then the sum of all $P_{i,IL}$ for the scheduling horizon should be zero. This implies that for the case of interruptible load $P_{i,IL}$ is strictly non-negative, while for the case of shifted load $P_{i,IL}$ can be either positive or negative. The voltage quality constraint for its magnitude at every bus, as also the loading limits of the lines and the transformers are given in (VIII). The power flow constraints are given in (IX) and (X).

To minimize the effect of demand charge pricing (DCP) the objective function and constraints are further updated and enhanced as follows:

minimize $$g = f + pk \cdot \sum_{\substack{i=[1,23],\\ j=i+1}} d_{i.j}$$ replaces ***(I)***

s.t. $$-[d_{i.j}] \le [P_{1,i} - P_{1,j}] \le [d_{i.j}]$$, for $i=[1,23]$ and $j=i+1$ ***(XI)***

Where:

pk: pareto shadow costs of quasi peak-shaving
d: slack variables
$P_{1,i}$: infeed bus (interconnection or slack) power at time i

This set-up essentially describes the aim to minimize the variance about the average of the overall feeder load that is served from the infeeding bus (numbered as bus 1), i.e. to minimize the peaks, by shifting them to valleys in a day-ahead horizon, and then throughout a billing period, since we are operating on a model predictive control manner. This approach reduces the effect of the DCP, since the DCP is employed at the highest hourly peak load of a feeder, hence, if all peaks are reduced by shifting them to the daily valleys, the DCP will be employed at a considerably reduced peak load. The set-up is not exhaustive and is not deterministic, in the sense that the value of *pk* will affect how much the daily load variance of the feeder will be reduced about its average. The higher the *pk*, the higher the “load smoothening” about its average.

Based on the overall optimal control formulation of the problem (I)-(XI) the consensus+innovations (C+I) based distributed control is obtained. C+I forms the basis of many agent-based distributed control architectures and can be roughly described in the form of the following iterative state (for example, device set points) updates:

$$x_n(k+1) = x_n(k) - \beta(k) \sum_{l \in \Omega} \left(x_n(k) - x_l(k) \right) + \alpha(k) \cdot \varepsilon(z_n)$$

where, $x_n(k+1)$ is the state of variable x by agent n at step k+1. This state os recursively updated by assimilating the k-step states of agents l belonging to the neighborhood Ω of agent n (the "Consensus" term), as also by a correction term ε, which is a function of local cost terms collected by agent n (the "Innovation" term). As one may notice, the aforementioned terms are accelerated by the corresponding time-varying gains β, α. Due to the iterative nature of the methodology, the gains have to be properly tuned to avoid instability (i.e. failure to converge to a desired state (control or set point)), as also for the state to converge in as few a number of steps as possible.

To determine the update terms of the C+I framework of the here proposed optimal control set-up for distribution networks, the Karush-Kuhn-Tucker (KKT) conditions have to be laid out; to extract the KKT conditions, the Lagrangian function of the above problem has to be first formulated. The focus will be on the coupled optimal power flow (COPF) problem, since all other constraints are linear and can be similarly extracted with the following process.

$$\begin{aligned}
L = & \sum_{i \in g} C\left(P_{g,i}\right) + \sum_{i \in B} \lambda_i \cdot \left[-P_{g,i} + P_{l,i} + \sum_{j \in NBi} \left(g_{ij} - b_{ij}\right) \cdot (\theta_i - \theta_j) \right] + \\
& + \sum_{i \in B} \mu_i \cdot \left\{ -Q_{g,i} + Q_{l,i} + \sum_{j \in NBi} \left[(\theta_i - \theta_j) \cdot \left(\frac{g_{ij}^2}{b_{ij}} - g_{ij} \right) + \frac{|v_i|}{b_{ij}} \left(-g_{ij}^2 - b_{ij}^2 \right) + \frac{|v_j|}{b_{ij}} \cdot \left(g_{ij}^2 + b_{ij}^2 \right) \right] \right\} + \\
& + \sum_{i \in g} u_{P,i} \cdot \left(P_{g,i} - P_{g,i,M} + T_{P,i}^2 \right) + \sum_{i \in g} l_{P,i} \cdot \left(-P_{g,i} + P_{g,i,m} + K_{P,i}^2 \right) + \\
& + \sum_{i \in g} u_{Q,i} \cdot \left(Q_{g,i} - Q_{g,i,M} + T_{Q,i}^2 \right) + \sum_{i \in g} l_{Q,i} \cdot \left(-Q_{g,i} + Q_{g,i,m} + K_{Q,i}^2 \right) + \\
& + \sum_{i \in B} u_{V,i} \cdot \left(V_i - V_{i,M} + T_{V,i}^2 \right) + \sum_{i \in B} l_{V,i} \cdot \left(-V_i + V_{V,i,m} + K_{V,i}^2 \right) + \\
& + \sum_{i \in B} \sum_{j \in NBi} u_{\ln,ij} \left\{ \left(g_{ij} - b_{ij}\right)^2 \cdot (\theta_i - \theta_j)^2 + \right. \\
& \left. + \left[(\theta_i - \theta_j) \cdot \left(\frac{g_{ij}^2}{b_{ij}} - g_{ij} \right) + \frac{|v_i|}{b_{ij}} \left(-g_{ij}^2 - b_{ij}^2 \right) + \frac{|v_j|}{b_{ij}} \cdot \left(g_{ij}^2 + b_{ij}^2 \right) \right]^2 - S_{ij,M}^2 + T_{l,ij}^2 \right\}
\end{aligned}$$

The resulting KKT conditions are:

$$\frac{\partial L}{\partial P_{g,i}} = 0 \Rightarrow \quad \frac{\partial C\left(P_{g,i}\right)}{\partial P_{g,i}} + \lambda_i + u_{P,i} - l_{P,i} = 0 \quad , \qquad \frac{\partial L}{\partial Q_{g,i}} = 0 \Rightarrow \quad \mu_i + u_{Q,i} - l_{Q,i} = 0 \quad ,$$

$$\frac{\partial L}{\partial \theta_i} = 0 \Rightarrow \quad \lambda_i \cdot \sum_{j \in NBi} \left(g_{ij} - b_{ij}\right) - \sum_{j \in NBi} \lambda_j \cdot \left(g_{ij} - b_{ij}\right) - \mu_i \cdot \sum_{j \in NBi} \left(g_{ij} + b_{ij}\right) + \sum_{j \in NBi} \mu_j \cdot \left(g_{ij} + b_{ij}\right) +$$

$$+ \sum_{j \in NBi} u_{\ln,ij} \left\{ 2\left(g_{ij} - b_{ij}\right)^2 \cdot (\theta_i - \theta_j) - \right.$$

$$\left. -2\left(\frac{g_{ij}^2}{b_{ij}} - g_{ij}\right) \cdot \left[(\theta_i - \theta_j) \cdot \left(\frac{g_{ij}^2}{b_{ij}} - g_{ij}\right) + \frac{|v_i|}{b_{ij}}\left(-g_{ij}^2 - b_{ij}^2\right) + \frac{|v_j|}{b_{ij}} \cdot \left(g_{ij}^2 + b_{ij}^2\right) \right] \right\}$$

$$+ \sum_{j \in B} u_{\ln,ji} \left\{ -2\left(g_{ji} - b_{ji}\right)^2 \cdot (\theta_j - \theta_i) + \right.$$

$$\left. +2\left(\frac{g_{ij}^2}{b_{ij}} - g_{ij}\right) \cdot \left[(\theta_i - \theta_j) \cdot \left(\frac{g_{ij}^2}{b_{ij}} - g_{ij}\right) + \frac{|v_i|}{b_{ij}}\left(-g_{ij}^2 - b_{ij}^2\right) + \frac{|v_j|}{b_{ij}} \cdot \left(g_{ij}^2 + b_{ij}^2\right) \right] \right\} = 0$$

$$\frac{\partial L}{\partial |v_i|} = 0 \Rightarrow \quad -\mu_i \cdot \sum_{j \in NBi} \frac{\left(g_{ij}^2 + b_{ij}^2\right)}{b_{ij}} - \sum_{j \in NBi} \mu_j \cdot \frac{\left(-g_{ij}^2 - b_{ij}^2\right)}{b_{ij}} + u_{V,i} - l_{V,i} +$$

$$+ \sum_{j \in NBi} u_{\ln,ij} \left\{ 2\frac{\left(-g_{ij}^2 - b_{ij}^2\right)}{b_{ij}} \cdot \left[(\theta_i - \theta_j) \cdot \left(\frac{g_{ij}^2}{b_{ij}} - g_{ij}\right) + \frac{|v_i|}{b_{ij}}\left(-g_{ij}^2 - b_{ij}^2\right) + \frac{|v_j|}{b_{ij}} \cdot \left(g_{ij}^2 + b_{ij}^2\right) \right] \right\}$$

$$+ \sum_{j \in B} u_{\ln,ji} \left\{ 2\frac{\left(g_{ij}^2 + b_{ij}^2\right)}{b_{ji}} \cdot \left[(\theta_i - \theta_j) \cdot \left(\frac{g_{ij}^2}{b_{ij}} - g_{ij}\right) + \frac{|v_i|}{b_{ij}}\left(-g_{ij}^2 - b_{ij}^2\right) + \frac{|v_j|}{b_{ij}} \cdot \left(g_{ij}^2 + b_{ij}^2\right) \right] \right\} = 0$$

$$\frac{\partial L}{\partial \lambda_i} = 0 \Rightarrow \quad -P_{g,i} + P_{l,i} + \sum_{j \in NBi} \left(g_{ij} - b_{ij}\right) \cdot (\theta_i - \theta_j) = 0$$

$$\frac{\partial L}{\partial \mu_i} = 0 \Rightarrow \quad Q_{g,i} - Q_{l,i} + \sum_{j \in NBi} \left[(\theta_i - \theta_j) \cdot \left(\frac{g_{ij}^2}{b_{ij}} - g_{ij}\right) + \frac{|v_i|}{b_{ij}}\left(-g_{ij}^2 - b_{ij}^2\right) + \frac{|v_j|}{b_{ij}} \cdot \left(g_{ij}^2 + b_{ij}^2\right) \right] = 0$$

$$\frac{\partial L}{\partial u_{P,i}} = 0 \Rightarrow \quad P_{g,i} - P_{g,i,M} + T_{P,i}^2 = 0, \qquad \frac{\partial L}{\partial l_{P,i}} = 0 \Rightarrow \quad -P_{g,i} + P_{g,i,m} + K_{P,i}^2 = 0,$$

$$\frac{\partial L}{\partial u_{Q,i}} = 0 \Rightarrow \quad Q_{g,i} - Q_{g,i,M} + T_{Q,i}^2 = 0, \qquad \frac{\partial L}{\partial l_{Q,i}} = 0 \Rightarrow \quad -Q_{g,i} + Q_{g,i,m} + K_{Q,i}^2 = 0,$$

$$\frac{\partial L}{\partial u_{V,i}} = 0 \Rightarrow \quad |v_i| - |v_{i,M}| + T_{V,i}^2 = 0, \qquad \frac{\partial L}{\partial l_{V,i}} = 0 \Rightarrow \quad -|v_i| + |v_{i,m}| + K_{V,i}^2 = 0$$

$$\frac{\partial L}{\partial u_{\ln,ij}} = 0 \Rightarrow \left(g_{ij} - b_{ij}\right)^2 \cdot (\theta_i - \theta_j)^2 + \left[(\theta_i - \theta_j)\left(\frac{g_{ij}^2}{b_{ij}} - g_{ij}\right) + \frac{|v_i|}{b_{ij}}\left(-g_{ij}^2 - b_{ij}^2\right) + \frac{|v_j|}{b_{ij}}\left(g_{ij}^2 + b_{ij}^2\right) \right]^2 - S_{ij,M}^2 + T_{l,ij}^2 = 0$$

$$\frac{\partial L}{\partial T_{P,i}} = 0 \Rightarrow \quad u_{P,i} \cdot T_{P,i} = 0, \qquad \frac{\partial L}{\partial K_{P,i}} = 0 \Rightarrow \quad l_{P,i} \cdot K_{P,i} = 0,$$

$$\frac{\partial L}{\partial T_{Q,i}} = 0 \Rightarrow \quad u_{Q,i} \cdot T_{Q,i} = 0, \qquad \frac{\partial L}{\partial K_{Q,i}} = 0 \Rightarrow \quad l_{Q,i} \cdot K_{Q,i} = 0,$$

$$\frac{\partial L}{\partial T_{V,i}} = 0 \Rightarrow \quad u_{V,i} \cdot T_{V,i} = 0, \qquad \frac{\partial L}{\partial K_{V,i}} = 0 \Rightarrow \quad l_{V,i} \cdot K_{V,i} = 0$$

$$\frac{\partial L}{\partial T_{\ln,ij}} = 0 \Rightarrow \quad u_{\ln,ij} \cdot T_{\ln,ij} = 0$$

The updated COPF in the C+I framework is now as follows:

$$\lambda_i(k+1) = \lambda_i(k) - \beta_\lambda \frac{\partial L}{\partial \theta_i} + \alpha_\lambda \frac{\partial L}{\partial \lambda_i}$$

$$\mu_i(k+1) = \mu_i(k) - \beta_\mu \frac{\partial L}{\partial |v_i|} + \alpha_\mu \frac{\partial L}{\partial \mu_i}$$

$$P_{g,i}(k+1) = \mathbb{P}\left(P_{g,i}(k) - \beta_P \cdot \left(\frac{\partial C(P_{g,i})}{\partial P_{g,i}} - \lambda_i(k+1) \right) \right) = \mathbb{P}\left(P_{g,i}(k) - \beta_P \cdot \left(2 \cdot a_g \cdot P_{g,i} + b_g - \lambda_i(k+1) \right) \right)$$

$$\theta_i(k+1) = \theta_i(k) - \beta_\theta \frac{\partial L}{\partial \lambda_i}$$

$$|v_i(k+1)| = |v_i(k)| - \beta_V \frac{\partial L}{\partial \mu_i}$$

$$Q_{g,i}(k+1) = \mathbb{P}\left(Q_{g,i}(k) + \beta_Q \cdot \mu_i(k+1) \right)$$

Where for subscripts:

i,j:	bus number,
g,l:	generator (set),
V:	voltage,
ln:	line,
NBi:	electric “neighborhood” of bus *i,*
m:	minimum allowable value (limit),
M:	maximum allowable value (limit),
B:	set of all buses,
λ, μ, u:	Lagrangian multipliers,

and for regular fonts:

C:	cost function,
P,Q,S:	active, reactive, apparent bus/line power,
|v|,θ:	bus voltage magnitude, angle,
g,b:	line conductance, susceptance,
λ, μ, u, l, T, K:	Lagrangian multipliers and factors,
α, β:	non-decaying C+I tuning parameter,

The update functions for the Lagrangian multipliers of the constraints on voltage magnitude and line capacity have been omitted for this part of the analysis, based on the

observations in Subtask 2.1, titled, “Network Design”, presented in “RPPR1 Q2 2016 7165” report of the second period of Year 1. To briefly remind those observations, voltage magnitude and line capacity limits of distribution feeders are not violated as of the design of those networks.

To analyze the convergence and performance of the COPF in the C+I framework, a stacked representation of the variables of the problem needs to be used. Hence, vector X is $X = [\lambda, \mu, V, \theta, P, Q]^{\mathsf{T}}$. As of this representation, the update functions presented above are also stacked accordingly and the iteration matrix G is:

$$G_{utr} = \begin{bmatrix} \lambda_1 & \lambda_2 & 0 & \lambda_3 & \lambda_4 & 0 \\ 0 & \mu_1 & \mu_2 & \mu_3 & 0 & \mu_4 \\ 0 & 0 & v_1 & v_2 & 0 & v_3 \\ 0 & 0 & 0 & \theta_1 & \theta_2 & 0 \\ p_1 & 0 & 0 & 0 & p_2 & 0 \\ 0 & q_1 & 0 & 0 & 0 & q_2 \end{bmatrix}$$

Where,

$$\lambda_1 = \mathrm{I} - \beta_\lambda \cdot [r(Y) - i(Y)]$$
$$\lambda_2 = \beta_\lambda \cdot [r(Y) + Y_{sqg}]$$
$$\lambda_3 = \alpha_\lambda \cdot [r(Y) - i(Y)]$$
$$\lambda_4 = -\alpha_\lambda \cdot \mathrm{I}$$
$$\mu_1 = \mathrm{I} + \beta_\mu \cdot Y_{sq}$$
$$\mu_2 = -\alpha_\mu \cdot Y_{sq}$$
$$\mu_3 = -\alpha_\mu \cdot [r(Y) + Y_{sqg}]$$
$$\mu_4 = -\alpha_\mu \cdot \mathrm{I}$$

$$v_1 = \mathrm{I} + \beta_V \cdot Y_{sq}$$
$$v_2 = \beta_V \cdot [r(Y) + Y_{sqg}]$$
$$v_3 = \beta_V \cdot \mathrm{I}$$
$$\theta_1 = \mathrm{I} - \beta_\theta \cdot [r(Y) - i(Y)]$$
$$\theta_2 = \beta_\theta \cdot \mathrm{I}$$
$$p_1 = \beta_P \cdot \mathrm{I}$$
$$p_2 = \mathrm{I} - \beta_P \cdot 2 \cdot a_g \cdot \mathrm{I}$$
$$q_1 = \beta_Q \cdot \mathrm{I}$$
$$q_2 = \mathrm{I}$$

Where,

I:	identity matrix,
r(z):	real part of element *z*,
i(z):	imaginary part of element *z*,
α, β:	acceleration parameters (*α*, *β* > 0),
Y:	admittance matrix,
Y_{sqg}:	a laplacian-type matrix where off-diagonal elements are $Y_{sqg,ij} = \frac{r(Y_{ij})^2}{i(Y_{ij})}$,
Y_{sq}:	a laplacian-type matrix where off-diagonal elements are $Y_{sq,ij} = -\frac{Y_{ij} \cdot Y_{ij}^*}{i(Y_{ij})}$

Assuming $P_g(0) = P_{g,min}$, $Q_g(0) = Q_{g,min}$ and λ and μ projected to the positive space. Then $[P_g(u)^{\mathsf{T}}\ Q_g(u)^{\mathsf{T}}] \geq [P_g(v)^{\mathsf{T}}\ Q_g(v)^{\mathsf{T}}]$ for any u > v, i.e. bounded monotonic sequences. Thus, G reduces to:

$$G_{utr} = \begin{bmatrix} \lambda_1 & \lambda_2 & 0 & 0 \\ 0 & \mu_1 & \mu_2 & \mu_3 \\ 0 & 0 & v_1 & v_2 \\ 0 & 0 & 0 & \theta_1 \end{bmatrix}$$

For the iterative procedure to converge, the spectral radius of G_{utr} needs to be strictly less than 1 [41]. Since, G_{utr} is a block upper triangular matrix, its eigenvalues are those of λ_1, μ_1, v_1 and θ_1. The eigenvalues of λ_1, μ_1, v_1 and θ_1 can be approximated according to the Bauer-Fike theorem (BFt) [42]. As of BFt, for any matrix M, that can be decomposed as $M = M_{utr} + M_{misc}$ if all elements of M_{misc} are less than ε, it is expected that:
$\rho(M) \leq \rho(M_{utr}) + O(\varepsilon)$
In this case, λ_1, μ_1, v_1 and θ_1 can each be decomposed as sums of an upper triangular and a second matrix with all the off-diagonal elements below the main diagonal (let the latter matrix be denoted as $lod(M)$). Hence, it is:

$$lod(\lambda_1) = -\beta_\lambda \cdot [r(Y) - i(Y)]$$
$$lod(\mu_1) = \beta_\mu \cdot Y_{sq}$$
$$lod(v_1) = \beta_V \cdot Y_{sq}$$
$$lod(\theta_1) = -\beta_\theta \cdot [r(Y) - i(Y)]$$

As of BFt, by properly selecting small β_x parameters, all elements of the aforementioned matrices can be reduced below an acceptable ε. For the upper triangular components of λ_1, μ_1, v_1 and θ_1 matrices, their eigenvalues are their diagonal elements, i.e.:

$$\lambda_{1,ii} = 1 - \beta_\lambda \cdot \left[\sum_{j \in NB_i} g_{ij} - \sum_{j \in NB_i} b_{ij} \right]$$
$$\mu_{1,ii} = 1 + \beta_\mu \cdot \sum_{j \in NB_i} \frac{Y_{ij} \cdot Y_{ij}^*}{b_{ij}}$$
$$v_{1,ii} = 1 + \beta_V \cdot \sum_{j \in NB_i} \frac{Y_{ij} \cdot Y_{ij}^*}{b_{ij}}$$
$$\theta_{1,ii} = 1 - \beta_\theta \cdot \left[\sum_{j \in NB_i} g_{ij} - \sum_{j \in NB_i} b_{ij} \right]$$

For strictly positive values of the acceleration parameters and any given power system of n buses, with line impedances $r_{ij}+j \cdot x_{ij}$, where r_{ij}, $x_{ij} > 0$, hence, $g_{ij} > 0$ and $b_{ij} < 0$, according to BFt $\boldsymbol{\rho(G_{utr}) < 1}$.

According to this analysis, it has been shown that the C+I implementation of the COPF converges, excluding the inequality constraints on the power quality limits. Furthermore, due to the fact that all update functions are linear combinations of continuous functions, the methodology converges to a fixed point [41]. From this and according to [43] the fixed point can be readily shown to be the optimal solution of the COPF problem.

For completeness, the proof of the COPF in the C+I framework is extended to account for the 'excluded' constraints. There are two update terms for the upper and lower limit of

the voltage magnitude and two for the maximum and minimum (essentially, bi-directional flow) line capacity limitation. All of these updates are of the same mathematical formulation, hence the proof for the upper limit of voltage constraints will be presented for simplicity. The update is reminded here:

$$u_{|v|,i}(k+1) = \mathbb{P}\left(u_{|v|,i}(k) + \beta_{|v|}\left(|v_i| - |v_{i,M}|\right)\right)$$

The projection of this update is to the positive space. Even if the projection was dropped, it is not possible to prove convergence according to [41] (i.e. ensuring that the spectral radius of the update/iteration matrix be strictly less than 1), because the diagonal element of $u_{|v|,i}$ is definitely equal to 1 and may not allow the corresponding eigenvalue to be reduced according to the Bauer-Fike theorem [42]. However, as from the "RPPR1 Q3 2016 7165" report of Q3 of Phase I of this project, let it be reminded that this update was extracted according to the Karush-Kuhn-Tucker conditions over the corresponding Lagrangian function of the COPF formulation, i.e. the above update function is, essentially:

$$u_{|v|,i}(k+1) = \mathbb{P}\left(u_{|v|,i}(k) + \beta_{|v|}\frac{\partial L}{\partial u_{|v|,i}}\right)$$

This update is of the gradient descent form [44]. Hence, if the above iterative function is bounded, it has a fixed point. In this sense, any positive number large enough may be chosen to project the above iteration in an up and down bounded space, thus, ensuring that the iterative process has a fixed point. Applying the same approach to the iterative function of the lower limit voltage, upper and lower limits of line capacity constraints and combining it with the proof of convergence of the rest of the update functions presented in the previous quarterly report, it is shown that the COPF formulation in the C+I framework converges to a fixed point. From this and according to [43] the fixed point can be readily shown to be the optimal solution of the COPF problem.

From the optimization problem described here it is easy to extend the proof of convergence to the scheduling problem presented in the whole (I)-(XI) set-up. This is due to the fact that the scheduling problem practically encapsulates the power flow formulation and adds inequality constraints, which, through the Lagrangian formulation of the dual problem and in the framework of the C+I approach, are expressed as iterative functions similar to the upper limit of voltage constraint presented right above. Hence, the optimal day-ahead scheduling problem in the C+I framework proves to converge to the optimal solution of the corresponding central formulation.

In the Appendix of this Task, we describe a heuristic method to improve the speed of convergence of the C+I methodology, which constitutes another contribution of our work of broader impact in the field of distributed, iterative solvers for optimization problems.

Three Milestones fell under this Task. Milestones M.1, M.7 and M.8. Milestone M.8 described, essentially, the improvements and the end-results of Milestone M.1, as the latter assessed the performance of the optimal control framework in the first stages of the project. Hence, Milestones M.1 and M.8 are described together. We conducted

exhaustive testing on three actual distribution feeders (two from the island of Rhodes in Greece, on from the island of Ikaria in Greece) and a test distribution feeder of 10-buses.

Milestones M.1 & M.8 (DELIVERED, SUCCESSFUL)

Average LCOE and cost analysis, Convergence Values

With regards to the testing of the control algorithm and the in-depth assessment of the simulated LCOE, the following major remarks were gathered:

- When there is no effort to minimize the DCP effect, the BSS is not used at all, but for cases that the PV power exceeds the load and would thus lead to inverse flows from the feeder upstream to the interconnection. According to most grid codes, this energy flow is not allowed and should, hence, be somehow mitigated.
- As from the analysis, there would be peak PV power leading to inverse energy flows for penetration of unit equipment installations in at least 50% of the end customers. The LCOE would be marginally below the $0.14/kWh threshold for such levels of penetration and all the way up to the case of 100% penetration that would exceed it.
- For the case of neglecting the effect of the DCP to the LCOE and unless some level of penetration of unit equipment installations leads to increased flows of power upstream to the interconnection (i.e. if the battery needs to be used to mitigate such phenomena) the LCOE is way above the $0.14/kWh threshold for high penetrations, since the effect of the DCP is not mitigated (the peaks are not reduced).
- For all cases that aim to reduce the effect of DCP to the LCOE, any increase in the cost-term consideration of the DCP reduces the LCOE.
- The LCOE can also be reduced if a policy of shared ownership is in place. Every end customer may sign a contract for a minimum amount of emergency charge of the battery storage for addressing extreme phenomena (black-outs, maintenance interruptions, weather causing damages to the grid, etc). This contractual agreement means that the user will pay an X% portion of the battery storage cost, thus discounting its operating cost from the optimization algorithm decision-making. The rest of the unit equipment cost (including the 100-X% of the storage capacity not paid by the said end customer) will be shared, though the cooperative acting as the aggregator, at a community level. In this case the results are updated as follows.
    - LCOE<$0.14/kWh for any level penetration, if the customer of the premises of the PV+BSS installations owns more than 25% of the system and expected IRR≤10%,
    - LCOE<$0.14/kWh for penetration up to 50% if the customer of the premises of the PV+BSS installations owns less than 25% of the system and expected IRR≤10%,
    - LCOE<$0.14/kWh for any level of penetration, if expected IRR≤10%
    - LCOE<$0.11/kWh for any penetration, if the customer of the premises of the PV+BSS installations owns more than 75% of the system,
    - LCOE<$0.11/kWh for penetration less than 40%, if the customer of the premises of the PV+BSS installations owns less than 50% of the system,

- LCOE<$0.11/kWh for penetration up to 16%, if the customer of the premises of the PV+BSS installations owns less 25% of the system,
- As IRR grows, the aforementioned penetrations that allow for the thresholds to not be exceeded, drop

Let it be here noted that the $0.14/kWh threshold is the one set by the SOPO of this project, while the $0.11/kWh threshold is the LCOE noted as before the deployment of any BTM PV+BSS, i.e. the energy billing per kWh without any contribution of resources. Journal paper submissions are under consideration.

Milestone M.7 (DELIVERED, SUCCESSFUL)

Distributed optimization algorithm convergence time

In this Milestone the convergence time of the C+I algorithm was sought to be assessed with a threshold of acceptable behavior 2s. Two distinctive outcomes should be commented. Firstly, regardless of the size of the feeder, the number of active resources and any random delays, the scheduling algorithm **would not** converge in time less than 2 s, if arbitrary initial values were assigned to the update terms. This implementation of the algorithm is also known as "cold start" and implies that there exists no prior knowledge of the state of the variables.

Secondly and, practically, since a "cold start" of the scheduling algorithm is not a realistic scenario, the "hot start" was also assessed. A "hot start" means that there exists (somehow) some knowledge about the update variables (usually from a previous step in a model predictive control approach) and either only one or two steps forward are added to the scheduling horizon or only some availability of resources is updated. For very few changes in the scheduling data of the algorithm, i.e. for "hot start" realization of the methodology, the metric of 2 s for time of convergence would be achieved. To quantify the premises of these tests, let it be noted that for the feeder R-23 of the island of Rhodes, Greece [45], with more than 50 load buses, presumably all equipped with active resources such as PV and storage, adding one step ahead in the scheduling horizon would not require more than 1.2 s average time to converge. Similarly, the convergence would be achieved in times around 1 s for an update in the PV forecast even of all buses. However, changing simultaneously the load and PV forecast beyond the deviations of most common forecasting tools would require considerable times to converge, as if it was a "cold start" implementation.

Appendix to Task 1

Cost of Battery Degradation

As long as lifetime affects the operational cost of a component and is in turn affected by the latter, that cost cannot be considered constant [46]. In the case of a battery storage system, degradation represents an actual operational cost since it translates to loss of capacity in the long term [47]. However, the loss of available capacity is in turn a function of the discharging cycles; i.e. the decision to operate it and at what level. The idea here proposed is that every discharge is averaged (in terms of used capacity) with the previous ones from the start of the battery operation system; dividing the total lifetime capacity of

the battery by this average, yields the lifetime, thus the effect of the use of the storage system on its operational cost. Assuming:

st: total hours from start of battery operation (in h),

A_{st}: total capacity of discharged Ah (or discharge cycles) from start of battery operation,

x or $P_{i,DCh,t}$: Next hour (*t+1*) discharge in Wh,

x/V_B: next hour discharge (in Ah, V_B: battery voltage across terminals)

Then the averaged usage profile is given by:

$$\frac{\left(A_{st} + x/V_B\right)\cdot 8760}{st+1} \text{ Ah/year (or discharges/year)}$$

Assuming a total of T_{Ah} of lifetime Ah then the lifetime of the battery is given as:

$$t = \frac{T_{Ah}\cdot(st+1)}{\left(A_{st} + x/V_b\right)\cdot 8760} \text{ years}$$

If C_0 is the capital cost of the battery (in $) and ***r%*** the expected/preferred internal return rate, then the Net Present Value [46] of the storage system would be:

$$NPV = C_0 - \sum_{i=1}^{t}\frac{C_i}{(1+r)^i} \Rightarrow (r\%: \textit{preferred IRR at end of } t, \textit{i.e.} NPV = 0) \Rightarrow$$

$$\Rightarrow \sum_{i=1}^{t}\frac{C_i}{(1+r)^i} = C_0 \Rightarrow (\textit{assuming yearly revenue } C_1 \cong C_2 \cong \ldots \cong C_t) \Rightarrow$$

$$\Rightarrow C_t \sum_{i=1}^{t}\left(\frac{1}{1+r}\right)^i = C_0 \Rightarrow (\textit{sum of geometric progression, } a_1 = \lambda = \frac{1}{1+r}) \Rightarrow$$

$$\Rightarrow C_t = C_0 \frac{1-\lambda}{\lambda\cdot\left(1-\lambda^t\right)}$$

Let it be noted that the assumed investment model represents the worst case scenario compared to accounting additionally for financial plan considerations. Furthermore, the cost calculation would be much more complicated and depend on parameters that should be approached only as specific study cases (out of the scope of the project).

Regarding the cost of degradation specifically, as of the specifications of any battery storage system, the battery capacity degrades by ***D%*** over ***Y*** lifetime cycles for ***d%*** DoD. That said for investment lifetime capacity T_{Ah}, the discharge degradation factor per capacity unit (recharged/discharged) is $(D^{1/TAh})/Ah$ and, thus, the available capacity $(1-D)^{1/TAh}/Ah$, which leads to the degradation cost per Ah recharged/discharged as:

$$C_{dgrdB} = C_0\cdot(1-D)^{1/T_{Ah}}\cdot\frac{x}{V_b}\cdot\frac{1-\lambda}{\lambda\cdot\left(1-\lambda^{\frac{T_{Ah}\cdot(st+1)}{\left(A_{st}+x/V_b\right)\cdot 8760}}\right)}$$

The above formulation clearly implies that if $A_{st} >> x$ (i.e. after a few dozens of recharge/discharge cycles or more), the C_{dgrdB} may be simplified and considered constant for longer periods of time and not be included as a function of the problem variables that would complicate the optimization. The exponent of λ, which is $\frac{T_{Ah} \cdot (st+1)}{\left(A_{st} + x/V_b\right) \cdot 8760}$ stands, as mentioned earlier, for the lifetime of the investment in years. Replacing the exponent with Y and calculating for various expected return rates r, it can be noticed that the inverse exponential term presents a rational function behavior, which may also be derived by:

$$\lambda^{Y} + \lambda^{Y-1} + ... + \lambda^{2} + \lambda^{1} \approx a \cdot Y$$

where, a is a parameter related to the preferred return rate r. This equation holds as of the Taylor series expansion of the left side of the equation for $\lambda \approx 1$, which is true for most common return rates r (ranging between 1-20%). That said the degradation cost per Ah may, thus, be reformulated as:

$$C_{dgrdB} = C_0 \cdot (1 - D)^{1/T_{Ah}} \cdot \frac{\left(A_{st} + x/V_b\right) \cdot 8760}{a \cdot T_{Ah} \cdot (st+1)} \qquad \textbf{(XII)}$$

An important point to be mentioned here is that we may not assume a specific lifetime Ah or cycles of the battery storage system (i.e. unknown credibility of value T_{Ah}), since as models of [48, 49] have shown, this approximation tends to overestimate (usually) or underestimate the battery storage lifetime (either this is expressed in time units or capacity in Ah) by an average of 10-15%, resulting to C_{dgrdB} variance in the ±14% interval, as this can be inferred by (XII). To this end, extensive tests on many battery storage systems of typical Li-ion technologies were executed by the project partner Aquion. It has been found that T_{Ah} may not be considered as a constant, but as a function of the operating temperature and the discharging profile. Assuming that the operating temperature may be kept somehow constant by proper (realistic) measures, the function of T_{Ah} is a linear approximation of the discharged energy per cycle as in:

$$T_{Ah} = -k \frac{\left(A_{st} + \sum_{t \in [1,t]} P_{i,DCh,t}/V_{b,t}\right) \cdot 24}{st + t} + m \qquad \textbf{(XIII)}$$

where, k and m are positive constants related to the battery technology. The averaging has been used, in order to weigh in the effect of the previous cycling behavior. As it can be noticed, there is an implicit assumption that only one full discharge occurs per day. Combining (XII, XIII) we get:

$$\sum_{t\in[1,24]} Dgd_{i,RCh,t} = \left[C_0 \cdot (1-D)^{1/T_{Ah}(P_{i,Dch,t})} \cdot \frac{\left(A_{st} + \sum_{t\in[1,t]} P_{i,DCh,t}/V_{b,t} \right) \cdot 8760}{a \cdot T_{Ah}\left(P_{i,DCh,t}\right) \cdot (st+t)} \right]^{T}_{t\in[1,24]} \cdot \left[P_{i,DCh,t}/V_{b,t} \right]_{t\in[1,24]} \quad (XIV)$$

With (XIV) and after the first few cycles of the BSS, we may use a constant degradation cost over every few dozens of cycles instead of optimizing in absolute detail.

Linearized Optimal Power Flow Equality Constraints for Resistive Aware Lines

We elaborate on the power flow constraints, since they represent significant contribution to the field. The original power flow $p_{ij} + i \cdot q_{ij} = v_i \cdot \left(v_i^* - v_j^*\right) \cdot y_{ij}^*$ equality constraint represents an equation that will render the optimization problem non-linear and non-convex, thus complicating its solution. For this purpose, we propose the following steps of linearization that take also into account the resistive nature of distribution feeders that are the ones serving the residentials customers at the core of our R&D.

- The power flow equality constraint can be rewritten in polar coordinates as

$$\left.\begin{aligned} p_{ij} &= g_{ij} \cdot |v_i|^2 - |v_i| \cdot |v_j| \cdot \left[g_{ij} \cdot \cos(\theta_i - \theta_j) + b_{ij} \cdot \sin(\theta_i - \theta_j) \right] \\ q_{ij} &= -b_{ij} \cdot |v_i|^2 - |v_i| \cdot |v_j| \cdot \left[g_{ij} \cdot \sin(\theta_i - \theta_j) - b_{ij} \cdot \cos(\theta_i - \theta_j) \right] \end{aligned}\right\} \quad (XV)$$

- All voltage magnitudes are close to 1 p.u., i.e. they may be set as $|v_i| = 1$,
- Voltage angle differences of neighboring buses in the system are small enough, so that (i) the resulting cosine is almost unitary and (ii) the difference practically occupies the nearly linear region of the sine function, i.e. $\cos(\theta_i - \theta_j) \cong 1$ and $\sin(\theta_i - \theta_j) \cong \theta_i - \theta_j$, respectively, and
- Conductances (resistances) are non-negligible compared to susceptances (reactances).

As from the above, (XI) is elaborated as:

$$\left.\begin{aligned} p_{ij} &= -b_{ij} \cdot (\theta_i - \theta_j) \\ q_{ij} &= -\cdot g_{ij} \cdot (\theta_i - \theta_j) \end{aligned}\right\} \Rightarrow \text{subtracting the bottom equation from the top one}$$

$$p_{ij} - q_{ij} = \left(g_{ij} - b_{ij}\right) \cdot (\theta_i - \theta_j) \quad (\textbf{XVI.a})$$

Since, by definition $g_{ij} + j \cdot b_{ij} = \dfrac{1}{r_{ij} + j \cdot x_{ij}}$ and $r_{ij}, x_{ij} \geq 0$, it follows that $b_{ij} \leq 0$ and $g_{ij} \geq 0$. This in turn means that the effect of line resistance to the calculation of the bus angles for any given dispatching is severe and at least as important as that of the reactance (or greater).

To offer a depiction of this observation let us recall that the power flow equality constraint of the classic DC OPF [37] is given by $p_{ij} = -b_{ij} \cdot (\theta_i - \theta_j)$

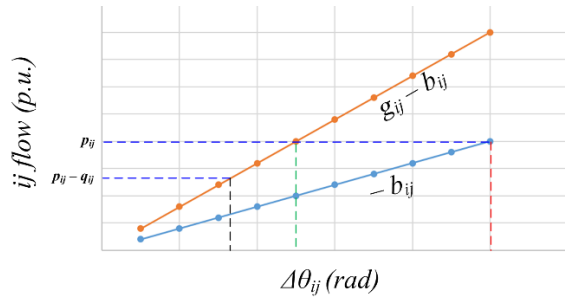

Fig. 2. Comparison of the effect of line resistance to the calculation of the angle difference in the linearized OPF formulation.

Following, see Fig. 2, where the vertical axis corresponds to the difference of the angles as a simple variable $\Delta\theta_{ij}$ (in *rads*) and the vertical axis represents power flows in per unit values. It is assumed that p_{ij} and q_{ij} are positive when flowing from bus i to bus j. Notice that for $|g_{ij}/\geq/b_{ij}|$ the magnitude of the slope of the line corresponding to the approximated power flow equality constraint according to (XVI.a) will be at least double of that of the classic DC OPF constraint. This, in turn, means that the angle difference for the same flow p_{ij} is, at most, half from that calculated based on the classic DC OPF. In fact, according to the above assumptions on the p_{ij} and q_{ij}, for generally inductively loaded distribution networks, the angle difference, as of (XVI.a) would be even smaller. To move further with the power flow equality constraint, the previously given assumptions on the angle differences and the lines conductance-susceptance relation are complemented by an additional assumption:

- All voltage magnitudes are close to 1 p.u., but only one multiplicative factor of $|v_i|$ may be set as $|v_i| = 1$,

This leads to (XV) being elaborated as:

$$\left.\begin{aligned} p_{ij} &= g_{ij} \cdot |v_i| - |v_j| \cdot g_{ij} - |v_j| \cdot b_{ij} \cdot (\theta_i - \theta_j) \\ q_{ij} &= -b_{ij} \cdot |v_i| - |v_j| \cdot g_{ij} \cdot (\theta_i - \theta_j) + |v_j| \cdot b_{ij} \end{aligned}\right\} \Rightarrow \quad p_{ij} \cdot g_{ij} - |v_i| \cdot g_{ij}^2 + |v_j| \cdot g_{ij}^2 = q_{ij} \cdot b_{ij} + |v_i| \cdot b_{ij}^2 - |v_j| \cdot b_{ij}^2$$

(***XVI.b***)

Due to the coupling of active and reactive power flows in the angle and voltage magnitude approximations of this set-up, we shall define these power flow formulation as Coupled Optimal Power Flow (COPF).

To assess the performance of the above formulation before proceeding to its distributed realization in the C+I framework, extensive tests were carried out. Indicatively, the comparative results for the OPF dispatching in a 10-bus radial system, including five DG units and nine load points is presented. The nominal capacity of the DG units in kW is given as vector in P_b = [0, 100, 50, 0, 150, 0, 0, 120, 100, 0]

The corresponding costs (as also of the in-fed energy through the slack bus) is considered linear and given as c = [0.276, 0.6797, 0.6551,0, 0.119,0,0, 0.3404, 0.5853, 0]

The active power demand required to be covered in kW is given per bus as

P_l = [0, -500, -200, -500, -300, -100, -200, -300, -500, -200]

assuming a power factor of 0.8 lagging. The dispatching results of the proposed decoupled OPF for distribution systems were identical to those of the classic decoupled OPF and read that the slack bus would cover 2650kW and the generator installed on the fifth bus would inject 150kW. Noticeable differences were observed between the voltage and angle outputs between the classic decoupled and the here proposed COPF, while the accurate solution as from the SDP relaxed OPF sets the benchmark.

Decoupled/DC OPF		**COPF**		**SDP-relaxed OPF**	
V in p.u.	Angle (rad)	V in p.u.	Angle (rad)	V in p.u.	Angle (rad)
1.0000	0	1.0000	0	1.0000	-0.0000
0.9959	-0.0056	0.9949	-0.0034	0.9950	-0.0024
0.9792	-0.0281	0.9744	-0.0171	0.9743	-0.0125
0.9762	-0.0322	0.9707	-0.0196	0.9705	-0.0144
0.9750	-0.0338	0.9693	-0.0205	0.9691	-0.0151
0.9731	-0.0365	0.9669	-0.0222	0.9667	-0.0164
0.9723	-0.0377	0.9658	-0.0230	0.9655	-0.0170
0.9708	-0.0398	0.9640	-0.0242	0.9637	-0.0180
0.9703	-0.0406	0.9633	-0.0247	0.9631	-0.0184
0.9700	-0.0410	0.9629	-0.0249	0.9626	-0.0185

Iteration gains for improved C+I convergence speed

To optimize the rate of convergence of the control algorithm for the scheduling problem in the C+I framework, the spectral radius of the iteration matrix of the updates of the algorithm had to be minimized. However, as it was noted earlier the reactive power of all buses and all inequality constraints are updated according to iterative functions with persistently unitary values across the diagonal of the iteration matrix. To this end, to optimize the rate of convergence of the algorithm of the scheduling problem in the C+I framework was updated as follows:

- Step 1: All iteration functions with persistently unitary values across the diagonal of the iteration matrix are dropped. As of this, the iteration matrix is reduced to:

$$G_{itop} = \begin{bmatrix} \lambda_1 & \lambda_2 & 0 & \lambda_3 & \lambda_4 \\ 0 & \mu_1 & \mu_2 & \mu_3 & 0 \\ 0 & 0 & v_1 & v_2 & 0 \\ 0 & 0 & 0 & \theta_1 & \theta_2 \\ p_1 & 0 & 0 & 0 & p_2 \end{bmatrix}$$

I.e. it consists only of the update terms of the COPF equality constraints of active and mixed active-reactive power multipliers (λ and μ, respectively), voltage magnitude, voltage angle and active power of active resources in the system.

- Step 2: As of the diagonal elements of G_{itop}, determine the minimum and maximum values for all "α_x" and "β_x" acceleration parameters (where x implies the corresponding update term) that limit the value of the diagonal elements between zero and one.
- Step 3: Exhaustively explore the available space of "α_x" and "β_x" acceleration parameters that minimizes the spectral radius of G_{itop} without allowing a zero eigenvalue.
- Step 4: Set all acceleration parameters of the iterative functions of the reactive power and the inequality constraints not included in Steps 2 and 3 above, equal to the minimum of all "α_x" and "β_x" acceleration parameters determined in Step 3.

Steps 1-3 follow the approach in [41], while Step 4 relies on the fact that these iterative functions will converge to the optimal solution, following the convergence rate of the rest of the updates.

Task 2: Software Implementation of Algorithms

• High-level description of research and outcomes: *Extensive load flow results on actual, distribution feeders showed that the network design is the major factor affecting power quality in terms of voltage deviations. The unit controller has been enabled with the control algorithm and tested in silico. Reliable controller-to-controller, controller-to-equipment, and controller-to-server communication have been developed and validated.*

Before deploying any control software in an actual system, concise in silico validation is required to foresee any unexpected outcomes or to fine tune the control software itself. The challenge of applying control algorithms at distribution systems is also relevant to the operating profile of the latter. Commonly, distribution feeders are designed to withstand loads that are projected in timelines of at least 10 years from the design phase, which implies that power quality concerns might not arise in the average case and any controls are solely improving energy profiles. This has been noted also by the OMF modeling of two cooperative distribution feeders from the US and three distribution feeders from islanded systems from Greece on the MATLAB platform.

Previous work conducted by NRECA on the GOSED project resulted in the creation of a Feeder Model, representing a portion of the CoServ Electric energy distribution system in Abilene Texas. This model represented two Feeders attached to the Aubrey Substation. These feeders are labeled "Aubrey 21" and "Aubrey 22". Using the climate information for Abilene Texas, and the SCADA data from the real feeder system for that time, the OMF calibration tool was used to modify the load objects in the Models to scale their output to match that of the real system. Indicative results from the voltage profiles of these two feeders are shown in the following figures.

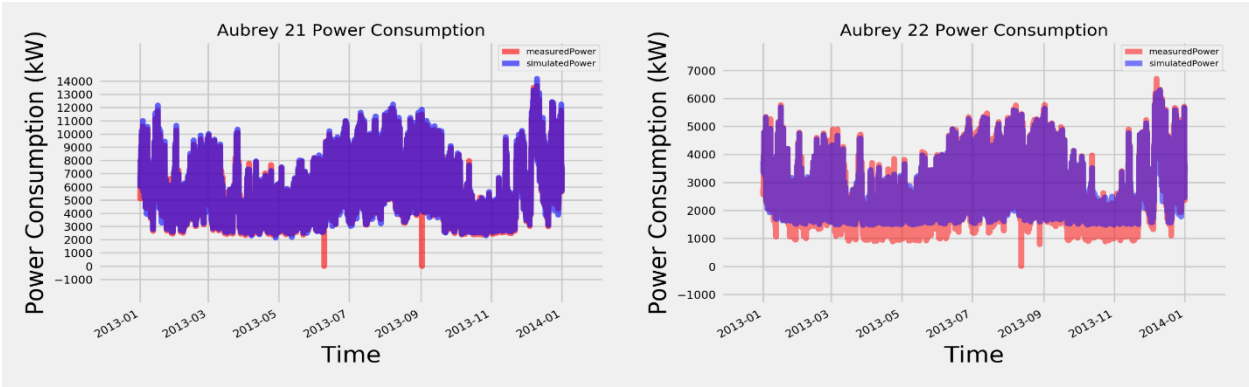

Fig. 3. OMF simulation and actual data of voltage from 2 cooperative feeders.

Fine tuning these feeder models to their actual metered data was successful, with deviations between actual and modeled feeder voltage profiles around 5% RMS. Following the adaptation of the actual feeder in its OMF representation, no results indicated any actual requirements for control with regards to power quality matters. In these feeders no RES or other DG assumptions/scenarios were tested. In the MATLAB platform, 3 feeders from Greece were modeled, 2 of the island of Rhodes (approximately 100 load buses each and installed load of 6 MW and 8 MW, respectively [45]) and one of the island of Ikaria (60 load buses, approximately 3.5 MW installed loads [50]). On these feeders, multiple PV penetration scenarios were tested. The two feeders of the island of Rhodes suffer from drop of voltage below 0.9 p.u. for loading above about 60% of the installed (or for photovoltaics penetration less than 40% at peak times) at any number of load buses among the first few from the in-feeding node. On the contrary, the distribution feeder of the island of Ikaria showed no drop or rise of voltage beyond limits regardless of the loading or the photovoltaics penetration at peak load times. The aforementioned data clearly depict that the network design is the major factor affecting power quality in terms of voltage deviations. In other words, if an aggregator or operator control the deployment of PV+BSS units, the voltage profiles will be maintained within limits, if not improved. However, such a policy cannot be considered as given, hence, optimal control of PV+BSS units is what may guarantee proper voltage profiles throughout all operating conditions and system constraints. Additionally, the test-bed of choice comprising units deployed on the CMU campus, is modeled in terms of energy interactions in the MATLAB platform, including also the actuation of the assets on the C+I framework. LCOE analysis performed in this last set-up largely confirmed the findings and analyses of Task 1.

In the same task, the control algorithm is incorporated on the controlling hardware that was initially a BeagleBoard and then a Raspberry Pi unit. In both cases a Linux-based operating system offered much flexibility for high level interaction (i.e. avoiding low-level automation) and set-up of the optimal control. Python is used to implement the C+I optimization algorithm, while ModBus is used to execute all electric energy control actions and collect measurements from the components. All data of operation and control of the PV+BSS systems are transmitted to a data repository and presented on a webpage for assessment of the overall test-bed. Some of the most important data that are being collected and formatted through the aforementioned host program are:

(i) load consumption per household, so as to assess the energy savings due to the control algorithm deployed,
(ii) battery storage used, so as to monitor lifetime capacity and assess timeline of replacement once depleted,
(iii) load and thermostat control activations, so as to assess the criticality of interruptible loads in the context of energy savings,
(iv) operating set-points of all control devices, so as to ensure the applicability of the control algorithm deployed.

Milestone M.2 (DELIVERED, SUCCESSFUL)

Simulated Data Accurate with Regards to Actual Measurements

The OMF model data has been tuned to match the actual feeder meter data as mentioned earlier with deviation less than the ±10% interval of RMS of the voltage profiles. By that it may be assured that there is capacity to model actual system data in simulation environments for the validation of control algorithms.

Milestone M.9 (SCOPE UPDATED, SUCCESSFUL)

Optimal Control Validated in a Simulated Feeder, Optimal Control on Controller

The CMU test-bed is modeled in the MATLAB platform, instead as a cooperative feeder in the OMF platform. The control algorithm is incorporated in that model. The LCOE analysis performed largely confirmed the theoretical findings and analyses of Task 1. More in-depth analysis of the LCOE performance and the performance of the distributed optimization framework on the OMF platform are being developed to yield additional *in silico* results for consideration.

Raspberry Pi units are used as the control device of the PV+BSS systems in the test-bed. All C+I controls, monitoring, logging and transmitting of data were coded in Python for the said device. In the following figure, the exchange of data among the Raspberry Pi for the control of the PV+BSS devices in indicatively shown for one agent.

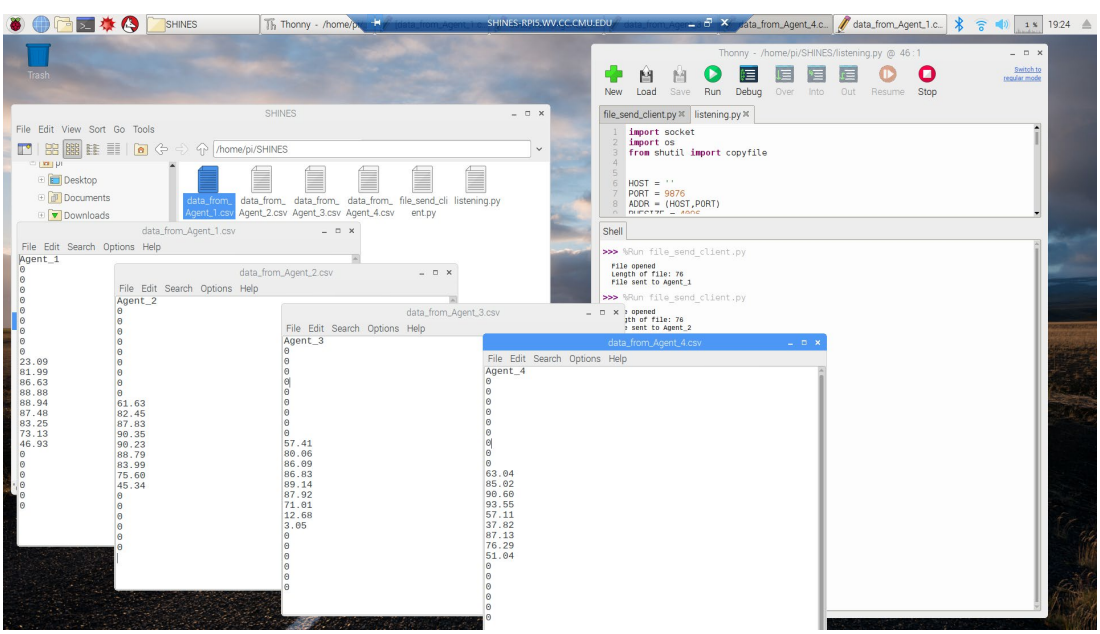

Fig. 4. Indicate output of control and operation of a RPi controller loaded with the C+I optimal control algorithm

Task 3: Cybersecurity Assurances

• High-level description of research and outcomes: *The focus is to identify and analyze potential attacks surfaces of the contextualized technology and provide security assurances based on implementing secure coding and communication standards and anomaly detection at the algorithmic and network levels. All security standards have been incorporated in the communication topology among the agents and the proof of convergence ensures guarantees that any behavior outside normal may be flagged as a malicious attack.*

Multiple coding paradigms for the software deployed on the test "unit" in the research facilities at CMU and the software to be developed and deployed on the test-bed, have been ascertained that meet standard (MultiSpeak™) interoperability and compliance standards. Secondly, we have investigated high-level resilience issues, specifically, the impact of adversarial data injections (inflicted by either malicious take-over of an agent or collection of agents and manipulating their update equations, or, compromising inter-agent communications at the network level) on the performance of the distributed algorithms. The results of this work in the more general context of distributed C+I based decision-making have been reported in a recent publication, see [51].

We also developed preliminary local online consistency check to detect a class of data injection attacks of the type described above. On the software implementation front, specifications are determined for static code inspection to identify possible code level vulnerabilities during on-site deployment. Further, for deployed software security assessment, we have made progress in setting up fault injection inputs and validation metrics for smart fuzz testing.

According to Milestone M.10 Secure Software Testing, two types of security concerns needed to be accounted for: the inter-device and the on-device attacks.

- Inter-device attacks are those that compromise the communication infrastructure between/among the controllers executing the control algorithm. In this context, and keeping in mind that the algorithm has been developed in the C+I framework, the information that needs to be shared between the controllers has been maliciously altered to not reflect the actual information transmitted originally by one/some controller(s). As from the formulation of the control problem, the controllers (seen as agents implementing the control algorithm) are not sharing physically any of the assets (battery, loads, PV of each end-customer), but only information on the Lagrangian multipliers of the equality constraints of the dual COPF formulation, voltage magnitudes and voltage angles. To this end, the control of the assets "under" any one controller cannot be directly affected by other controllers, but only the information of the exchanged variables.
- On-device attacks are considered, those that compromise the measuring and control topologies connected to the system controllers or the system controller as a whole. By that, it is expected that either the measurements are maliciously elaborated to read

different values than the actual ones or the control actions are not realized as calculated by the control algorithm or a combination of the previous two attacks or the system controller is set (somehow) offline.

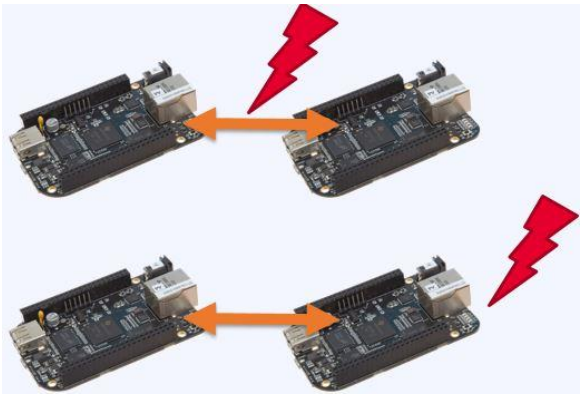

Based on the aforementioned analysis we propose the following security protocol that alerts for threats and averts specific attacks in the C+I framework of optimal control.

Cyber Security Protocol for ABC4PV C+I based Control Algorithm

IF control does not converge (average rate plus overhead) => raise flag/warning => Steps 2 & 3, ELSE keep checking convergence rate at error changes

IF all data exchanges not-constant => Attack is of inter-device type => Step 4 & 5

IF some data exchanges constant/missing => On-device attack or point malfunction => Step 4 & 6

Charge battery storage to contracted level for each end-user. Revert to default inverter operation. Message reporting to server.

Split control set (all feeder) in groups by binary search, until inter-device attacks isolated. Message reporting to server. => Step 7.

Group control points excluding nodes of constant/missing information. => Message reporting to server. => Step 7.

Determine new Cyber Security monitoring groups as per splits in Steps 5 or 6.

Milestone M.3 (DELIVERED, SUCCESSFUL)

Designing Secure IT Framework for C+I Optimal control

The specific Milestone needed to be revisited later in Period 3, although it was initially delivered in Period 1. The reason had to do with the change of test-bed and the different requirements set by each framework. This is by itself an important note that needs to be considered for actual cases. There is no one secure protocol for IT infrastructure and processes, and different vendors, users and aggregators will prefer different solutions. All the interactions among the agents in the control topology were conducted over internet protocols with no provision of security. In order to properly test the cyber security of the

control topology the IT department at CMU advised to upgrade the communication protocols to REST/HTTP. Representational State Transfer (REST) is a software architecture describing framework for creating Web services. These Web services, RESTful Web services (RWS), provide interoperability between computer systems on the Internet. RWS facilitates textual representations of Web resources, which is in the case of this project the representation for measurement, information and control messages across the agents of the proposed platform. REST has from its conception also incorporated a few security design principles that serve for improved performance overall, such as reduced privileges of entities over functions, prefer-to-deny access as default setting, and validation of access requests to mention a few [52].

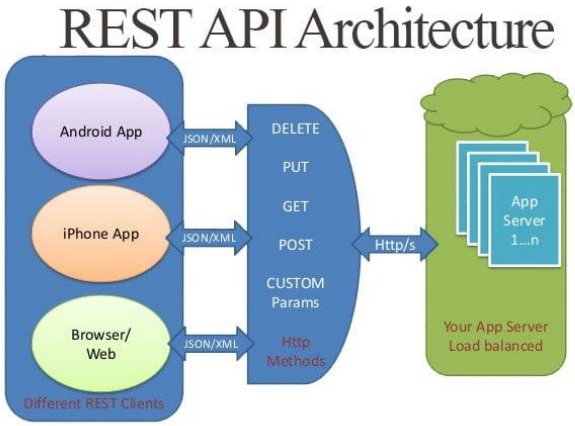

Milestones M.10 & M.14 (DELIVERED, SUCCESSFUL)

Secure Software Testing and Cybersecurity Assessment

The C+I framework itself as shown earlier must converge to a solution and, thus, any malicious attack will not allow that. Hence, the control algorithm is inherently secure and will be able to easily identify cyber intrusions of inconsistent data. The protocol of flags/warning and corrective measures given in the protocol earlier, in light of the tests conducted is submitted as a deliverable. Additionally, the results of Milestone M.3 complement the secure IT framework. Let some important remarks be mentioned here:

- The radial structure of distribution feeders greatly accommodates the efficacy of the proposed protocol, since the exchange of updated data in the C+I algorithmic framework occurs only between electrically connected nodes.
- Any split of the control group of nodes in the feeder will also be of radial structure, thus, the sub-groups security is also ensured.
- The binary type of search in implementing the splits (see Fig. 5) ensures a fast method to isolate inter-device attacks.

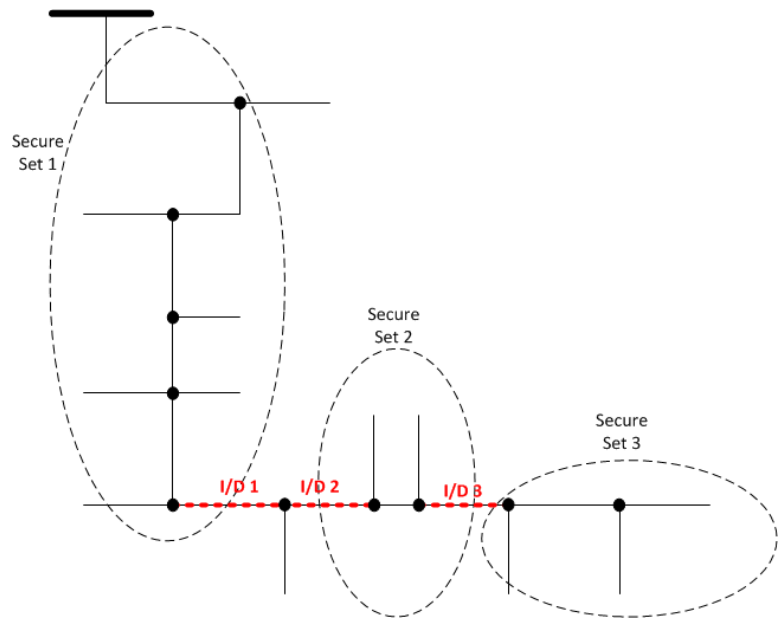

Fig. 5. Employed splits at the occurrence of a security alert for an intra-device attach on the optimal control

- The charging of the battery storage systems at the end customers' installations needs to be executed in case there is a generalized attack that could lead to further severe system occurrences, hence the end-customers must be able to serve their emergency loads.

Task 4: Installation of Physical Components and Test-bed Setup

• High-level description of research and outcomes: *The project testbed built in the context of the project consists of 6 networked ABC4PV units deployed on CMU campus, Pittsburgh. Specifically, a set of 4 building roofs were identified that host 6 PV+BSS systems throughout the said facilities.*

The CMU campus in Pittsburgh, PA, comprises buildings of commercial type (libraries, classrooms, offices, etc.) with relatively constant daytime load curves and very low valleys in the weekday nights and weekends, as also of residential type (mainly dorms) with peaking loads around afternoon and early night times all days. The campus area spans 6 million square feet, thus, representing topological scarcity among the buildings and geographical terrain variety, due to the rocky profile of Pittsburgh area. The microclimate is relatively interesting in the context of Photovoltaic generation with longer winters and fewer sunny days than other parts of the country.

Given the requirement for diverse attributes in the types of loads of the test-bed, the CMU campus was an ideal option for the deployment of the equipment conceptualized and designed as a "unit" in the framework of the ABC4PV. By properly selecting the locations in the campus where the units are deployed, the challenge of ensuring uninterrupted communication among sufficiently distant control points and testing the set-up against cyber-security threats were realistically assessed. This analysis also offered insight on how the research conducted in this project can behave in an actual setting

without any loss of generality. In the following 3 photos the locations of the PV+BSS installations may be noted.

Fig. 6. Locations of the SHINES/ABC4PV test-bed of six PV-BSS units on CMU campus, Pittsburgh

The final Bill of Materials for the “unit” that each PV+BSS system would describe is given in the following tables.

PV Subsystem

Item	*Description*	*Manufacturer*	*Part #*
1,1	PV Module	Trina	TSM-280DD05A.05
1,2	Racking	Rooftech	RT-[E]
1,3	Optimizer	Tigo	Tigo TS4-R-O
1,4	Tigo Gateway	Tigo	CloudConnect Advanced
1,5	Tigo Comms	Tigo	Gateway included
1,6	Arc Fault Detection	DC Sunvolt	ADU - Arc Fault Detection Module
1,7	Array Disconnect contactor		
1,8	Box for arc fault		

Battery Subsystem

Item	*Description*	*Manufacturer*	*Part #*
2,1	Battery	SimpliPhi	SimpliPhi-PHI-3.4
2,2	Battery Wall Racks		

Power Electronics Subsystem

Item	*Description*	*Manufacturer*	*Part #*
3,1	Inverter	Schneider	Conext XW+ 5548-NA
3,2	Power Distribution Panel	Schneider	Conext XW+ PDP
3,3	Charge Controller	Schneider	XW-MPPT80-600
3,4	Control Panel	Schneider	Conext 865-1050-01
3,5	Comms Panel	Schneider	Conext 865-1058 ComBox
3,6	Battery Monitor	Schneider	Conext 865-1080-01
3,7	100A DC Breaker	Schneider	865-1070

The differences between an actual cooperative feeder and the CMU test bed are briefly discussed here, in light of their effect to the R&D results of our work. Firstly, photovoltaic and battery storage systems installed behind the meters of customers (broadly speaking) with energy consumptions of equal or greater kWh amounts may not affect the power quality of the respective feeders. Voltage rise (frequent occurrence in feeders which are highly penetrated by photovoltaic systems) may not be noticeable, since all photovoltaic energy is balanced by the (at least) equal load demand. Although the optimal control algorithm may cater for the regulation of voltage deviations beyond the power quality standards, the mind-set behind the design of the “units” falls in the above description. Secondly, a main promise by the optimal control algorithm is the energy savings procured by shifting the photovoltaic energy of all “units” in the feeder (through the battery storage systems) to times of the day that will help smooth out the peak of the feeder and, thus, reduce peak demand charges. However, in any practical feeder comprising, at least, a few hundreds of houses, deploying any number of “units” below a total of 30-40% penetration (at peak load) will have unobservable, if not zero, effect in the aforementioned scope. To this end, the reconfiguration of the test-bed from a cooperative feeder to 6 “units” on 4 different CMU campus locations did not affect the outcomes of the research.

Milestones M.4 & M.5 (DELIVERED, SUCCESSFUL)

Test-bed Selection and Physical Unit Design

The reasons for selecting CMU as the test-bed of the project were just described. With regards to the unit design, beyond the bill of materials, the schema in Fig. 7 of the system design is offered as the overall single line diagram of the deployed equipment.

Milestone M.6 (DELIVERED, SUCCESSFUL)

Test-bed Simulation Analysis

The CMU test-bed was simulated in the MATLAB platform and, beyond the long-term energy dispatching, the convergence performance was also assessed. The convergence fell into the thresholds of less than 2s implementation of the commands, thanks to the distributed set-up of the C+I algorithm; we indicatively show the cold start convergence

with arbitrary initial conditions in the following two figures for dispatching of PV energy and in-feeding energy from the slack-bus. As for the energy dispatching, the LCOE results are identical to those gathered in Task 1. Indicatively, we show the convergence for the test bed in one of the autumn months in 2019 in Fig. 8.

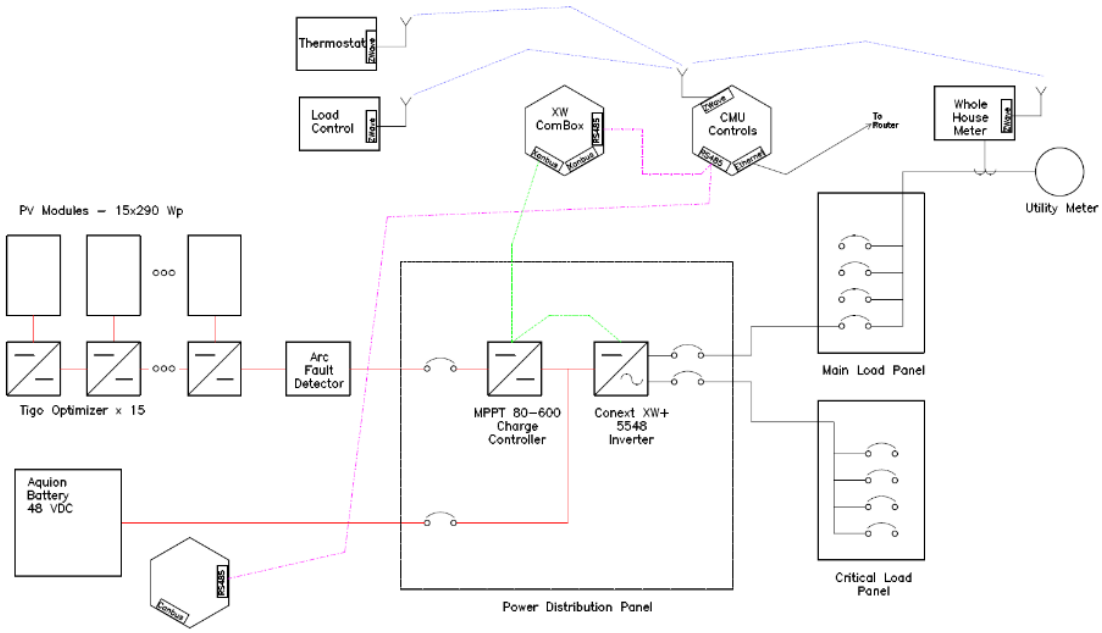

Fig. 7. Single-line electric diagram of each PV-batter unit in the SHINES/ABC4PV test-bed on CMU campus, Pittsburgh.

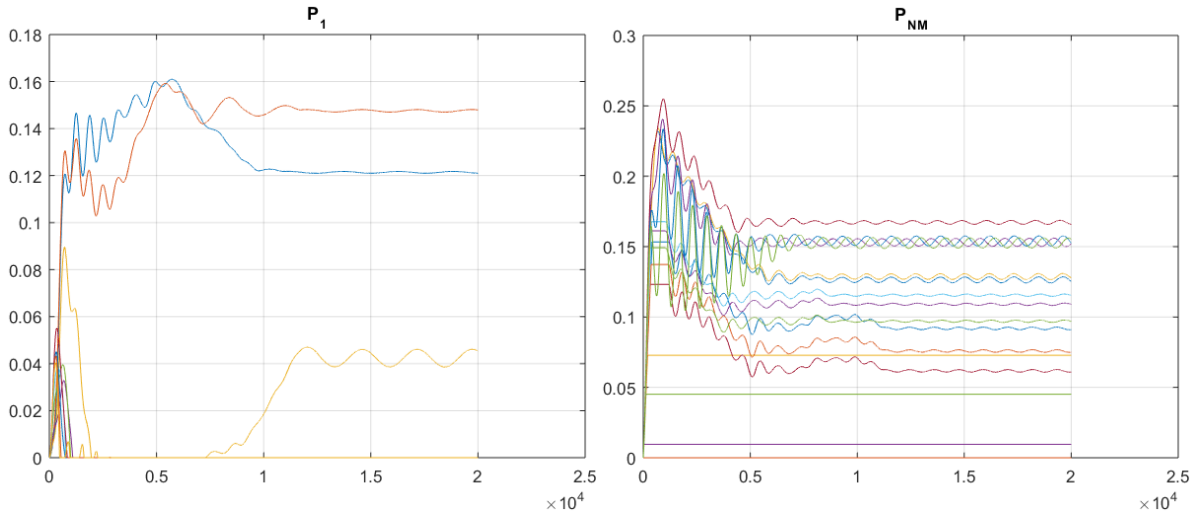

Fig. 8. Convergence in control set-points of demand response from interruptible loads and PV generation for the test-bed on an autumn day in 2019.

As for the components themselves, the tests we conducted with the inverter and the BSS systems showed that the execution command from the controller to the converter occurred in less than 1s, while the BSS response between 40%-50% of DoD and 100%-0% DoD were 1' and less than 60', respectively. These results confirm the timely response of the unit controller and components for flexible operation under various conditions.

Fig. 9. Deployment of the PV, BSS and control equipment in the test-bed at the CMU campus, Pittsburgh.

Milestone M.11 (DELIVERED, SUCCESSFUL)

Full Deployment and Validation

The photos in Fig. 9 show the various stages of the PV+BSS systems deployment, installation and operation at the CMU test-bed.

Further to the deployment of the PV+BSS units themselves, a concise SAM analysis was conducted. In that analysis however, there were considerable restrictions in the assumptions that could be inputted and the analysis that could be, thus, made. Five different US locations were assessed, while also a probabilistic analysis was attempted. From the bulk of results the following conclusions were drawn. Without any tax credits and assuming that each residential user is responsible for purchasing the equipment for his/her household, the threshold of 0.14 $/kWh of LCOE cannot be achieved under almost any circumstances. This observation further validates part of the policy proposal that the project consortium has previously described. The unit equipment ownership should be shared among the end users in a feeder, as that could be a cooperative in the paradigm studied throughout this work. Moreover, the matter of tax credits should be considered based on an alternative policy understanding. In the cooperative paradigm discussed in this project, there are certain demand charge pricing policies for peak loads. This is essentially an approach to mitigate high loads occurring in a small time frame in a day and rather be shifted to other times of the day, throughout the billing horizon which is, usually a month. By properly charging storage devices from PVs, loads can be served in a way that peaks are filling the daily valleys, thus reducing the effect of demand charging. In the described set-up, the unit equipment is not purposed for investment aims, but rather

as a facilitator of the energy shifting between the hours of the day. By further using the cooperative organization of end-users, the proposed approach can be more easily justified.

As for the convergence of LCOE results across platforms, compared to the SAM output of 17.29 $c/kWh, the 14 $c/kWh that seeks to minimize the demand charging pricing effect the deviation is within the errors of accounting for network costs that the MATLAB analysis has not included to the extent that SAM analysis does. Although the requirements of the respective Milestone sought for 5% error between the methods, this 20% error without network and billing costs, may be considered adequately acceptable.

Task 5: Performance Testing in Test-bed

• High-level description of research and outcomes: *All challenges that might lead to out-of-ordinary behavior of the unit have been identified and an operating protocol for the default operation is being prepared.*

Two types of operation are identified and are planned to be handled accordingly. Normal operation and operation under IT failures. To properly design the default operation of all units in the proposed control framework multiple questions need to be answered concerning the possible operating scenarios. They are listed as follows:

1. How fast does algorithm run?
2. What data needs to be collected?
3. How many data periods should be collected locally?
4. How long should this be stored?
5. How often should data be uploaded to the server?
6. What happens if a period is missed?
7. What format is used to send data?
8. Does the controller have a reset? (i.e., if a loop does not report over a certain period, there is a software and/or hardware reset of the controller?)
9. Is data pushed from the controller to the cloud, or fetched by the cloud? If the former, how to prevent collisions? If the latter, how does the controller respond to a fetch request – is there some sort of interrupt or is it built into the main algorithm?
10. How is data stored in cloud? Structured database?
11. Are external datasets such as temperature, co-op load, NEISO load, Co-op goals, etc.) required?
12. How is data accessed?
13. Who has access to cloud data? Read/write permissions?
14. Is there a program in the cloud that does calculations and formats data into reports? Format of report?
15. How are error messages reported?
16. Is there a web interface for the co-op to review data and set goals?
17. What is being done with the data after it is collected?
18. Can the controller firmware be updated remotely?
19. How to verify that firmware was installed correctly. What happens if an update fails?
20. If a piece of equipment needs to be reset (controller, Schneider controls, inverter, MPPT controller, circuit breaker, etc.) what is the procedure?

21. Does the customer have any access to the data generated by the unit controller?
22. Does the customer have access to any data available through the unit equipment?

According to these concerns the protocol of normal operation and alerts is put together.

Normal Operation Protocol and Alerts

Default Operation Protocol for ABC4PV Control Strategy (per M.5 numbering)

1. Any execution time beyond the 2 s threshold should raise a warning flag. Further info in Cyber Security Protocol of operation Textbox Ph.2-3.
2. All energy data.
3. 15-minute intervals data will be collected from energy meters.
4. Flush/message/email server in 15-minute intervals. Clear cache every one-day ahead scheduling interval.
5. See (4).
6. Missed flush/message/email update of data signals some type of control point failure. Further info in Cyber Security Protocol of operation Textbox Ph.2-3.
7. Txt files formatting used for data transmission.
8. Manual restart available. Automatic restart available. All functions resume execution.
9. Receive/deliver receipts are available through the communication protocol of the controllers.
10. (tbd by server set-up)
11. No external data are required for the control framework.
12. Data on server is accessed through secure connection. Data on controllers is accessed through remote desktop application.
13. Username/password protected access to all data access end-points is ensured.
14. Formatting is realized on the server receiving the controller data.
15. Message reporting is emailed to control administrator.
16. Server equipped with a web interface.
17. Data is stored locally to server.
18. Control firmware updated remotely as per (12).
19. Manual checks on code updates on controllers. Automation at commercial level

For the case of operating under communication failures, multiple tests needed to be conducted and assess the behavior of the control platform. The following scenarios were accounted for.

1) Communication failure at the methodology-level. For this type of failure three sub-scenarios were considered:
   a) The communication failure is a loss of signal.
   b) The communication failure is a network breakdown.
   c) A combination of (a) and (b) failures.
2) Communication failure at the controlled assets level. Two sub-scenarios were considered here:
   a) Failures on sensors.
   b) Failures on actuators.
3) Lastly, combinations of all above communication failures were considered.

Based on all above mentioned scenarios exhaustive tests were conducted on the MATLAB platform, as also with the Raspberry Pis as the control hardware of the test-bed. It was noted that for none of the above failures would the test-bed not optimize a control strategy either locally or within a subset of controlled assets. In the simulation environment it was noted that only for great numbers of communication breakdowns or method failure (cyber attacks considered equivalently here), would the overall strategy delay in deciding a new control point, or, at least, raising a flag of erroneous operation.

At this point let it be noted that the following webpage will offer visual output of the most recent operating and control data of the ABC4PV test-bed: https://cms-staging.andrew.cmu.edu/energy-2/research-innovation/shines-testbed.html

Milestones M.12 & M.15 (DELIVERED, SUCCESSFUL)

Normal Operation Performance and Performance Under Communication Failures

All hot-start control actions are reached after a small number of C+I method iterations that take less than 2s to converge, while the actuation is within the 1s threshold. Voltage concerns were not noticed and could not be tested in the test-bed set-up of CMU. When communication fails, various degrees of local optimality may be noted. The convergence and actuation times are not violated, nevertheless, the global optimum is evidently not achieved.

Task 6: Energy Storage Sub-System and Full System Assessment and Control Optimization

• High-level description of research and outcomes: *Our policy and PV+BSS proposal from Task 1 was repeated here for various practical reasons. The battery tests confirmed the approximations of battery life and its effects in the overall control methodology as perceived in Task 1.*

At this point, we will not repeat our proposal about policy and ownership that achieves LCOE below the $0.14/kWh threshold as analyzed in Task 1, since the results are the same. Given the fact that the test-bed of the CMU campus could not offer us full control of a feeder and detailed logging of its costs of operation as a whole, we cannot confirm with certainty the policy proposal. However, our publications are under review by policy experts and we expect updates on our estimates and alternatives ideas on our assumptions. Nevertheless, it is relatively valuable to show how, after the departure of BSS manufacturer partner Aquion from the project consortium and the unavoidable change of battery type, capacity and technology how the tests on the new battery compare with our assumed battery lifetime model in Task 1. As it may be seen in the Fig. 10, the inverse proportional linear model of lifetime of a BSS as its cycle DoD increases is valid and may be considered as a good estimate for longer term resource scheduling assessments.

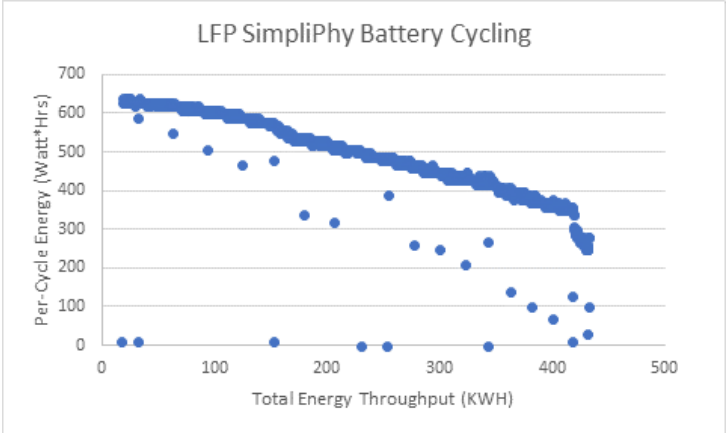

Fig. 10. Test results confirming an inverse linear model of battery lifetime on maximum available capacity per cycle.

Milestone M.13 (SCOPE UPDATED, SUCCESSFUL)

Test-bed LCOE and Voltage Profile Simulation Assessment

Within the MATLAB platform we were able to model the CMU campus test-bed as an energy entity and assess its LCOE. The said LCOE was approximately equal to the LCOE calculations from the SAM platform. However, we were not able to validate voltage profiles since the electric topology of the CMU campus would be particularly complicated for modeling, while the effect of the deployed PV+BSS units would be negligible to make sense to compare and analyze. Voltage profile assessment with regards to simulations, although hardly expected to be affected, might be a concern in some very extreme cases of system deployments.

Milestones M.17 (DELIVERED, SUCCESSFUL)

Final Report and Optimal Control Software

This document serves as the field report for the CMU test-bed, ranging from its design in terms of equipment, the controls, the policy proposal that could be implemented in an actual feeder, and the process of deploying and controlling the PV+BSS assets. The optimal control code was prepared and is executed in Python and is available at a CMU repository for other users to assess and use. It is compliant with ModBus protocol of actuation for converters and controllable switches.

Milestones M.18 (SCOPE UPDATED, SUCCESSFUL)

Test-Bed models in MATLAB, OMF and SAM

The CMU test-bed model has been implemented in full in MATLAB and SAM and is at a CMU repository for other users to assess and use. All LCOE and other benchmark values have been achieved and some insights were considered in a policy framework that we proposed.

Significant Accomplishments and Conclusions

This project led to three major accomplishments, of significant practical and theoretical value, in the field of behind-the-meter (BTM) PV penetration in distribution systems as well as their efficient control and coordination. These are stated below:

1. With regards to “cost of PV energy”, the first major result is that the LCOE for PV+BSS systems may be kept under the $0.14/kWh LCOE threshold in setups where the overall cost function takes into account the savings procured when managing the effects of demand charge pricing. By attempting to reduce the daily variance of the load about its average for all loads along a feeder, the effect of demand charge pricing is minimized. The effect can be so significant that the cost for served load pre- and after- the installation of PV+BSS systems may be the same for certain penetrations and ownership shares of PV+BSS systems among the feeder/cooperative users.

2. It has been vastly discussed that PV revenues usually benefit middle-to-high income brackets, because of the considerable capital expenses in buying the equipment. To this end, this project proposes a policy of shared ownership, that is structurally equivalent to the cooperative paradigm. In this paradigm, the residential customer at whose premises the PV+BSS system is installed, may incur some capacity contraction in the event of emergency situations; likewise, it benefits from the energy savings procured by these assets.

3. With regards to optimal control synthesis and implementation, the consensus+innovations based distributed approach provides scalability and robustness. The algorithms developed are further hardware agnostic and requires modest computation and communication at the agents. The agent-based distributed paradigm developed in this project paves the way for large-scale distributed energy management and dispatch and largely avoids the pitfalls of classical cloud-based centralized decision-making architectures that are highly sensitive to communication and computation bottlenecks.

Inventions, Patents, Publications, and Other Results

In the course of this project, we published the following papers:

1. Y. Chen, S. Kar, and J.M.F. Moura. "Resilient Distributed Field Estimation." *SIAM Journal on Control and Optimization* 58, no. 3 (2020): 1429-1456.
2. G. He, R. Ciez, P. Moutis, S. Kar, and J.F. Whitacre. "The economic end of life of electrochemical energy storage." *Applied Energy* 273 (2020): 115151.
3. Y. Chen, S. Kar, and J. M. F. Moura, “Resilient distributed estimation: Sensor attacks”, *IEEE Transactions on Automatic Control*, vol. 64, no. 9, pp. 3772–3779, Nov. 2019.
4. Y. Chen, S. Kar, and J. M. F. Moura, “Resilient distributed parameter estimation with heterogeneous data”, *IEEE Transactions on Signal Processing*, vol. 67, no. 19, pp. 4918–4933, Oct. 2019.
5. G. He, D. Zhang, X. Pi, Q. Chen, S. Kar, and J. Whitacre, “Spatiotemporal arbitrage of large-scale portable energystorage for grid congestion relief”, in 2019 IEEE Power & Energy Society General Meeting (PESGM), IEEE, 2019,pp. 1–5.
6. P. Moutis , G. Hug, and S. Kar , “Resistive Aware Linear Approximations for Solving the Optimal Power Flow Problem for Distribution Networks”, in 2019 Sustainable Power & Energy Conference (iSPEC)), Beijing, 2019.
7. G. He, Q. Chen, P. Moutis, S. Kar, and J. F. Whitacre, “An intertemporal decision framework for electrochemical energy storage management”, Nature Energy, vol. 3, no. 5, pp. 404–412, Apr. 2018.
8. S. Weerakkody, B. Sinopoli, S. Kar, and A. Datta. "Information flow for security in control systems." In *2016 IEEE 55th Conference on Decision and Control (CDC)*, pp. 5065-5072.

Path Forward

Although the key SUNSHOT and SHINES objectives of $0.14/kWh and $0.11/kWh LCOE thresholds were achieved for BTM PV+BSS systems under the considered framework, we believe that BTM assets may have additional revenue streams of particularly high value. Namely, the contracts of availability we mentioned in our policy proposal, could be properly quantified and included in the LCOE. That could account for further cost improvement, which is a subject of ongoing and future research.

Storing energy for emergency situations is equivalent to pricing the absence of energy in the event of a system disruption. In this sense, we need to quantify the value of emergency load serving according to classical approaches. One of them is to use the cost of typical fuels used most regularly for emergency generator sets. In a broader sense, we could also attempt to quantify the value of keeping the lights on at fire stations, police stations, hospitals and other critical infrastructure of that kind. These potential costs/savings, when properly accounted for in our dispatch objectives, could provide quantifiable savings as well as more realistic control solutions.

Another important effort is to scale up the consensus+innovations based distributed control solutions to multi-agent test cases of at least 1000 control points. Based on our theoretical and test findings, the convergence time of the model-predictive decisions will be scale gracefully with the number of agents and almost independent of disruptions in the operating environment such as emergency events, network reconfigurations and plug-and-play.

The research team is already pursuing funding opportunities from SETO and elsewhere, in order to continue working on the aforementioned research directions.

At the same time, the project team is exploring opportunities of shaping the battery industry, by interacting with think tanks that focus especially on the utilization of electric vehicle batteries. Specifically, the team is focusing on unlocking new value streams by combining vehicle-to-grid services by electric vehicles with effective PV integration and utilization achieved by robust optimal control frameworks of the type developed in this project. By leveraging our ongoing work, we can affect the BSS competition and market deployments in a meaningful way.

References

[1] Lazard, "Levelized Cost of Energy Report," ed, 2019.
[2] J. P. Fossati, A. Galarza, A. Martín-Villate, J. M. Echeverría, and L. Fontán, "Optimal scheduling of a microgrid with a fuzzy logic controlled storage system," *International Journal of Electrical Power & Energy Systems,* vol. 68, pp. 61-70, 2015.
[3] Q. Jiang, M. Xue, and G. Geng, "Energy management of microgrid in grid-connected and stand-alone modes," *IEEE transactions on power systems,* vol. 28, no. 3, pp. 3380-3389, 2013.
[4] M. H. Moradi, M. Abedini, and S. M. Hosseinian, "A combination of evolutionary algorithm and game theory for optimal location and operation of DG from DG owner standpoints," *IEEE Transactions on Smart Grid,* vol. 7, no. 2, pp. 608-616, 2015.
[5] R. Palma-Behnke *et al.*, "A microgrid energy management system based on the rolling horizon strategy," *IEEE Transactions on smart grid,* vol. 4, no. 2, pp. 996-1006, 2013.
[6] D. Guasch and S. Silvestre, "Dynamic battery model for photovoltaic applications," *Progress in Photovoltaics: Research and applications,* vol. 11, no. 3, pp. 193-206, 2003.
[7] S. S. Reddy and J. A. Momoh, "Realistic and transparent optimum scheduling strategy for hybrid power system," *IEEE Transactions on Smart Grid,* vol. 6, no. 6, pp. 3114-3125, 2015.
[8] W. Shi, X. Xie, C.-C. Chu, and R. Gadh, "Distributed optimal energy management in microgrids," *IEEE Transactions on Smart Grid,* vol. 6, no. 3, pp. 1137-1146, 2014.
[9] N. Li, L. Chen, and S. H. Low, "Optimal demand response based on utility maximization in power networks," in *2011 IEEE power and energy society general meeting*, 2011: IEEE, pp. 1-8.
[10] J. Soares, H. Morais, T. Sousa, Z. Vale, and P. Faria, "Day-ahead resource scheduling including demand response for electric vehicles," *IEEE Transactions on Smart Grid,* vol. 4, no. 1, pp. 596-605, 2013.
[11] Z.-f. Tan, L.-w. Ju, H.-h. Li, J.-y. Li, and H.-j. Zhang, "A two-stage scheduling optimization model and solution algorithm for wind power and energy storage system considering uncertainty and demand response," *International Journal of Electrical Power & Energy Systems,* vol. 63, pp. 1057-1069, 2014.
[12] Z. Wang, B. Chen, and J. Wang, "Decentralized energy management system for networked microgrids in grid-connected and islanded modes," *IEEE Transactions on Smart Grid,* vol. 7, no. 2, pp. 1097-1105, 2015.
[13] Y. Xiang, J. Liu, and Y. Liu, "Robust energy management of microgrid with uncertain renewable generation and load," *IEEE Transactions on Smart Grid,* vol. 7, no. 2, pp. 1034-1043, 2015.
[14] Z. Yang, R. Wu, J. Yang, K. Long, and P. You, "Economical operation of microgrid with various devices via distributed optimization," *IEEE Transactions on Smart Grid,* vol. 7, no. 2, pp. 857-867, 2015.
[15] M. D. Hopkins, A. Pahwa, and T. Easton, "Intelligent dispatch for distributed renewable resources," *IEEE Transactions on Smart Grid,* vol. 3, no. 2, pp. 1047-1054, 2012.
[16] N. Zhang, Z. Hu, D. Dai, S. Dang, M. Yao, and Y. Zhou, "Unit commitment model in smart grid environment considering carbon emissions trading," *IEEE transactions on smart grid,* vol. 7, no. 1, pp. 420-427, 2015.
[17] E. Sortomme, M. M. Hindi, S. J. MacPherson, and S. Venkata, "Coordinated charging of plug-in hybrid electric vehicles to minimize distribution system losses," *IEEE transactions*

on smart grid, vol. 2, no. 1, pp. 198-205, 2010.

[18] L. Jian, H. Xue, G. Xu, X. Zhu, D. Zhao, and Z. Shao, "Regulated charging of plug-in hybrid electric vehicles for minimizing load variance in household smart microgrid," *IEEE Transactions on Industrial Electronics,* vol. 60, no. 8, pp. 3218-3226, 2012.

[19] S. Weckx and J. Driesen, "Load balancing with EV chargers and PV inverters in unbalanced distribution grids," *IEEE Transactions on Sustainable Energy,* vol. 6, no. 2, pp. 635-643, 2015.

[20] B. Sun, Z. Huang, X. Tan, and D. H. Tsang, "Optimal scheduling for electric vehicle charging with discrete charging levels in distribution grid," *IEEE Transactions on Smart Grid,* vol. 9, no. 2, pp. 624-634, 2016.

[21] Z. Wang and S. Wang, "Grid power peak shaving and valley filling using vehicle-to-grid systems," *IEEE Transactions on power delivery,* vol. 28, no. 3, pp. 1822-1829, 2013.

[22] Z. Tan, P. Yang, and A. Nehorai, "An optimal and distributed demand response strategy with electric vehicles in the smart grid," *IEEE Transactions on Smart Grid,* vol. 5, no. 2, pp. 861-869, 2014.

[23] S.-K. Moon and J.-O. Kim, "Balanced charging strategies for electric vehicles on power systems," *Applied Energy,* vol. 189, pp. 44-54, 2017.

[24] M. L. Crow, "Electric vehicle scheduling considering co-optimized customer and system objectives," *IEEE Transactions on Sustainable Energy,* vol. 9, no. 1, pp. 410-419, 2017.

[25] L. Zhang, F. Jabbari, T. Brown, and S. Samuelsen, "Coordinating plug-in electric vehicle charging with electric grid: Valley filling and target load following," *Journal of Power Sources,* vol. 267, pp. 584-597, 2014.

[26] Z. Hu, K. Zhan, H. Zhang, and Y. Song, "Pricing mechanisms design for guiding electric vehicle charging to fill load valley," *Applied Energy,* vol. 178, pp. 155-163, 2016.

[27] E. R. Muñoz, G. Razeghi, L. Zhang, and F. Jabbari, "Electric vehicle charging algorithms for coordination of the grid and distribution transformer levels," *Energy,* vol. 113, pp. 930-942, 2016.

[28] K. Valentine, W. G. Temple, and K. M. Zhang, "Intelligent electric vehicle charging: Rethinking the valley-fill," *Journal of Power Sources,* vol. 196, no. 24, pp. 10717-10726, 2011.

[29] K. Zhan, Z. Hu, Y. Song, N. Lu, Z. Xu, and L. Jia, "A probability transition matrix based decentralized electric vehicle charging method for load valley filling," *Electric Power Systems Research,* vol. 125, pp. 1-7, 2015.

[30] R. Olfati-Saber, J. A. Fax, and R. M. Murray, "Consensus and cooperation in networked multi-agent systems," *Proceedings of the IEEE,* vol. 95, no. 1, pp. 215-233, 2007.

[31] A. G. Dimakis, S. Kar, J. M. Moura, M. G. Rabbat, and A. Scaglione, "Gossip algorithms for distributed signal processing," *Proceedings of the IEEE,* vol. 98, no. 11, pp. 1847-1864, 2010.

[32] Z. Zhang and M.-Y. Chow, "Convergence analysis of the incremental cost consensus algorithm under different communication network topologies in a smart grid," *IEEE Transactions on Power Systems,* vol. 27, no. 4, pp. 1761-1768, 2012.

[33] S. Kar and G. Hug, "Distributed robust economic dispatch in power systems: A consensus+ innovations approach," in *Power and Energy Society General Meeting, 2012 IEEE*, 2012: IEEE, pp. 1-8.

[34] S. Yang, S. Tan, and J.-X. Xu, "Consensus based approach for economic dispatch problem in a smart grid," *IEEE Transactions on Power Systems,* vol. 28, no. 4, pp. 4416-4426, 2013.

[35] G. Binetti, A. Davoudi, D. Naso, B. Turchiano, and F. L. Lewis, "A distributed auction-based algorithm for the nonconvex economic dispatch problem," *IEEE Transactions on Industrial Informatics,* vol. 10, no. 2, pp. 1124-1132, 2014.
[36] S. Kar, G. Hug, J. Mohammadi, and J. M. Moura, "Distributed State Estimation and Energy Management in Smart Grids: A Consensus ${+} $ Innovations Approach," *IEEE Journal of Selected Topics in Signal Processing,* vol. 8, no. 6, pp. 1022-1038, 2014.
[37] J. A. Taylor, *Convex optimization of power systems*. Cambridge University Press, 2015.
[38] T. Esram and P. L. Chapman, "Comparison of photovoltaic array maximum power point tracking techniques," *IEEE Transactions on energy conversion,* vol. 22, no. 2, pp. 439-449, 2007.
[39] E. F. Camacho and C. B. Alba, *Model predictive control*. Springer Science & Business Media, 2013.
[40] A. Campoccia, L. Dusonchet, E. Telaretti, and G. Zizzo, "Comparative analysis of different supporting measures for the production of electrical energy by solar PV and Wind systems: Four representative European cases," *Solar Energy,* vol. 83, no. 3, pp. 287-297, 2009.
[41] Y. Saad, *Iterative methods for sparse linear systems*. SIAM, 2003.
[42] T. Kato, *Perturbation theory for linear operators*. Springer Science & Business Media, 2013.
[43] J. Mohammadi, G. Hug, and S. Kar, "Agent-Based Distributed Security Constrained Optimal Power Flow," *IEEE Transactions on Smart Grid,* 2016.
[44] D. P. Bertsekas, "Nonlinear programming," *Journal of the Operational Research Society,* vol. 48, no. 3, pp. 334-334, 1997.
[45] P. Moutis, P. Georgilakis, and N. Hatziargyriou, "Voltage Regulation Support Along a Distribution Line by a Virtual Power Plant Based on a Center of Mass Load Modeling," (in English), *Ieee Transactions on Smart Grid,* Article vol. 9, no. 4, pp. 3029-3038, JUL 2018 2018, doi: 10.1109/TSG.2016.2624633.
[46] S. C. Myers and N. S. Majluf, "Corporate financing and investment decisions when firms have informationthat investors do not have," National Bureau of Economic Research, 0898-2937, 1984.
[47] H. Ibrahim, A. Ilinca, and J. Perron, "Energy storage systems—Characteristics and comparisons," *Renewable and sustainable energy reviews,* vol. 12, no. 5, pp. 1221-1250, 2008.
[48] D. U. Sauer and H. Wenzl, "Comparison of different approaches for lifetime prediction of electrochemical systems—Using lead-acid batteries as example," *Journal of Power sources,* vol. 176, no. 2, pp. 534-546, 2008.
[49] H. Bindner, T. Cronin, P. Lundsager, J. F. Manwell, U. Abdulwahid, and I. Baring-Gould, *Lifetime modelling of lead acid batteries*. 2005.
[50] P. Moutis and N. D. Hatziargyriou, "Decision trees-aided active power reduction of a virtual power plant for power system over-frequency mitigation," *IEEE Transactions on Industrial Informatics,* vol. 11, no. 1, pp. 251-261, 2015.
[51] Y. Chen, S. Kar, and J. M. Moura, "Adversary detection and resilient distributed estimation of parameters from compact sets," *arXiv preprint arXiv:1701.00878,* 2017.
[52] J. H. Saltzer and M. D. Schroeder, "The protection of information in computer systems," *Proceedings of the IEEE,* vol. 63, no. 9, pp. 1278-1308, 1975.